Rivista Italiana di Paleontologia e Stratigrafia
(*Research in Paleontology and Stratigraphy*)
vol. 131(1): 177-200. **March 2025**
DOI: https://doi.org/10.54103/2039-4942/23142

CORAL CARBONATE PRODUCTION DURING THE PALEOCENE: INSIGHTS FROM THE MAIELLA MASSIF (PENNAPIEDIMONTE, CENTRAL ITALY)

GIOVANNI COLETTI[1*], LUCREZI COMMISSARIO[2], MUBASHIR ALI[1], LUCA MARIANI[3], BRUNO GRANIER[4], MARCO BRANDANO[5], ALESSANDRO MANCINI[5], GIOVANNI RUSCIADELLI[6,7], CRISTIANO RICCI[7], JUAN IGNACIO BACETA[9], GUILLEM MATEU-VICENS[8] & DANIELA BASSO[1]

[1]Dipartimento di Scienze dell'Ambiente e della Terra, Università degli Studi di Milano-Bicocca, Piazza della Scienza 1, 20126, Milano, Italia. E-mail: giovanni.coletti@unimib.it; m.ali17@campus.unimib.it; daniela.basso@unimib.it
[2]School of Biological, Earth and Environmental Sciences, University College Cork, Distillery Fields, T23 N73K, North Mall, Ireland. E-mail: luc.commissario@gmail.com
[3]Dipartimento di Scienze Chimiche e Geologiche, Università di Modena e Reggio Emilia, Via Giuseppe Campi 103, 41125, Modena, Italia. Email: l.mariani35@unimore.it.
[4]Département des Sciences de la Terre et de l'Univers, Faculteé des Sciences et Techniques, Université de Bretagne Occidentale, Avenue Le Gorgeu 6, CS 93837, F-29238, Brest, France. E-mail: bruno.granier@univ-brest.fr.
[5]Dipartimento di Scienze della Terra, Università di Roma la Sapienza, Piazzale Aldo Moro 5, 00185, Roma, Italia. E-mail: marco.brandano@uniroma1.it; a.mancini@uniroma1.it.
[6]Dipartimento di Ingegneria e Geologia, Università di Chieti-Pescara, Via dei Vestini, Campus Universitario, 66100, Chieti, Italia. E-mail: grusciadelli@unich.it.
[7]Strata GeoResearch, Via dei Vestini 31, 66100, Chieti, Italia. E-mail: c.ricci2737@gmail.com.
[8]Interdisciplinary Ecology Group, Universitat de les Illes Balears, Cra. de Valldemossa, Km. 7.5, 07122 Palma de Mallorca, Spain. E-mail: guillem.mateu@uib.es.
[9]Department of Stratigraphy and Paleontology, The University of the Basque Country, E48940 Leioa, Bizkaia, Spain. E-mail: juanignacio.baceta@ehu.eus.
*****Corresponding author.

Associate Editor: Francesca Bosellini.

To cite this article: Coletti G., Commissario L., Ali M., Mariani L., Granier B., Brandano M., Mancini A., Rusciadelli G., Ricci C., Baceta J.I., Mateu-Vicens G. & Basso D. (2025) - Coral carbonate production during the Paleocene: insights from the Maiella massif (Pennapiedimonte, Central Italy). *Rivista Italiana di Paleontologia e Stratigrafia,* 131(1): 177-200.

Keywords: Reefs; calcareous algae; rudists; shallow-water carbonates; Late Cretaceous; Danian; Thanetian.

Abstract. The succession of the Maiella massif is analyzed, focusing on the colonial-coral bearing deposits occurring just below and immediately above the Cretaceous/Paleogene boundary. The Upper Cretaceous material is dominated by rudists and larger benthic foraminifera with a significant contribution from colonial corals. In the Lower Paleocene, the first two groups are absent and colonial corals dominate the skeletal assemblage. This supports the hypothesis of a good recovery of colonial corals carbonate production following the end Cretaceous extinction and their overall resilience. Similar to modern reefs, Lower Paleocene bioconstructions have a framework dominated by corals and red calcareous algae. However, unlike modern reefs, micrite makes up the vast majority of the internal sediment, suggesting a development into a low-energy environment. Compared to Upper Paleocene coral boundstones, those from the Lower Paleocene of Maiella display a higher abundance of corals, suggesting a reduction in coral carbonate production during the Late Paleocene. This decline is also reflected by a period of scarcity of coral-dominated facies throughout the Tethys, starting from the latest Paleocene and extending till the end of the Middle Eocene. This can be connected to global temperatures, which rise in the Thanetian and remain relatively high till the end of the Middle Eocene, however, other factors most likely played a role. The quantitative analysis of the skeletal assemblage turns out to be a useful instrument for tracking the effect of environmental changes. Further data, especially from long and extensive successions of neritic carbonates such as those of Maiella, may help in disentangling the effects of the other environmental variables.

Received: April 29, 2024; accepted: January 13, 2025

Introduction

Tropical coral reefs account for approximately one-sixth of Earth's coastlines, representing one of the most biologically diverse shallow-marine ecosystems in the ocean and providing invaluable ecosystem services for millions of people (Birkeland 1997; Paulay 1997; Moberg & Folke 1999; Knowlton et al. 2010). Most of these biogenic structures are directly threatened by human activities and by bleaching events driven by rising temperatures (Bryant et al. 1998; Wilkinson 2004; Bellwood et al. 2006; Descombes et al. 2015; Cheung et al. 2021). Scleractinian corals, and the bioconstructions they develop, have existed since the Triassic and managed to survive even during rapid and catastrophic events such as the Cretaceous/Paleogene extinction (Flügel & Flügel-Kahler 1992; Moussavian & Vecsei 1995; Wood 1995; Vecsei & Moussavian 1997; Kiessling et al. 1999; Kiessling & Baron-Szabo 2004; Pomar & Hallock 2008; Pandolfi & Kiessling 2014; Kiessling & Kocsis 2015). Coral bioconstructions are also documented for most of the Cenozoic, including during global warming events (e.g., Zamagni et al. 2012; Pomar et al. 2017; Bosellini et al. 2022; Martin-Martin et al. 2023; Ali et al. 2024). This suggests that coral bioconstructions are an overall resilient ecosystem, able to endure both catastrophic events and prolonged periods of unfavorable conditions over the geological time/space scale. Although they might be quite resilient, the features of these bioconstructions can change over time in response to environmental stressors. In order to gain insights over the potential long-term effects of global warming on these structures, several papers have analyzed the evolution and distribution of corals, bioconstructions, and coral-bioconstructions through time (e.g., Wood 1995; Kiessling et al. 1999, 2003; Bosellini & Perrin 2008; Johnson 2008; Morsilli et al. 2012; Stolarski et al. 2016; Pomar et al. 2017; Cornacchia et al. 2021; Benedetti et al. 2024; Cipriani et al. 2024). This research effort highlighted major trends, but also uncertainties and gaps of knowledge. It has been suggested that coral bioconstructions might have significantly changed their ecological niche during the Cenozoic (Pomar & Hallock 2007, 2008; Pomar et al. 2012, 2017). Some authors noted the complex relationship between the distribution of corals and temperature (Bosellini & Perrin 2008; Coletti et al. 2022). Others discussed the connection between building capacity and biodiversity, highlighting how the latter sometimes is positively coupled with the former (Bosellini et al. 2021) and sometimes it is not (Johnson et al. 2008). However, the lack of quantitative data on fossil carbonate deposits, particularly on their skeletal assemblages, severely hinders our ability to compare fossil coral bioconstructions and rigorously test the various hypotheses regarding their evolution through time (Kiessling et al. 1999; Coletti et al. 2022; Bialik et al. 2023).

Bioclastic sediments and bioconstructions, ranging in age from the Jurassic to the Miocene (Crescenti et al. 1969; Vecsei et al. 1998, Rusciadelli et al. 2003), are exposed along the flanks of the Maiella massif in Central Italy, offering a unique window into the evolution of these carbonate-producing environments. Within the 'Vallone delle Tre Grotte' (VTG, from here onward), in the basal breccia of the Santo Spirito Formation, there are boulders and blocks of coral-boundstone, lying right above Upper Cretaceous, rudist-rich, bioclastic carbonates (Vecsei 1991; Moussavian & Vecsei 1995; Vecsei & Moussavian 1997; Vecsei et al. 1998) (Fig. 1). These blocks are remnants of coral bioconstructions that developed shortly after one of the main biotic crises of the Phanerozoic (the K/Pg extinction) and before the latest Paleocene – Early Eocene warm interval, a period of global decline in the abundance of coral-dominated bioconstructions (Kiessling et al. 1999; Scheibner & Speijer 2008; Zamagni et al. 2012; Pandolfi & Kiessling 2014; Kiessling & Kocsis, 2015; Aguilera et al. 2020; Pomar et al. 2017; Coletti et al. 2022). The main goal of this paper is thus to provide an updated analysis of the skeletal assemblages of these coral-dominated bioconstructions initially described by Vecsei (1991), Moussavian & Vecsei (1995), and Vecsei & Moussavian (1997). More accurate descriptions of the outcrops and their position within the VTG are provided, including details on the lithostratigraphic units immediately below and above the investigated interval. The microfacies are analyzed in detail, providing a quantitative framework to describe and compare the investigated Paleocene bioconstructions, first with the underlying Upper Cretaceous bioconstructions, and then with other Paleocene bioconstructions of the Tethys. This comparison, based on the quantitative features of the skeletal assemblage, is subsequently used to better understand the effects of Late Paleocene warming on coral-dominated bioconstructions.

Geological setting

The Maiella massif, situated in Central Apennines (Fig. 1A-B), represents the northernmost part of the Apulian Carbonate Platform, a thick carbonate sequence developed from the Jurassic to the Miocene in the interior of Adria (Eberli et al. 1993; Bernoulli et al. 1996; Vecsei & Moussavian 1997; Vecsei et al. 1998; Nicolai & Gambini 2007; Rusciadelli & Di Simone 2007; Sani et al. 2016; Vitale & Ciarcia 2022) (Fig. 1C-E). The latter is a northern promontory of the African Plate, that collided with the Eurasian Plate following the closure of the Alpine Tethys during the Alpine orogenesis (Muttoni et al. 2013) (Fig. 1D). The successions exposed in the Maiella massif span from the Jurassic to the Miocene and can be divided into various units (Crescenti et al. 1969; Accarie 1988; Moussavian & Vecsei 1995; Vecsei & Moussavian 1997; Vecsei et al. 1998) (Fig. 1E, F).

The oldest exposed units are the Upper Jurassic to upper Albian carbonates deposited in both shallow (Morrone di Pacentro Formation) and deep-water settings (Fig. 1) (Vecsei et al. 1998; Rusciadelli & Di Simone 2007; Eberli et al. 2019). These limestones are capped by a karst surface with bauxitic soils testifying a prolonged period of subaerial exposure (late Albian - early Cenomanian) (Fig. 1). The period of platform exposure was followed by the formation of a deep and steep escarpment (paleoescarpment), abruptly separating the platform in the south from the basin in the north (Crescenti et al. 1969; Accarie 1988; Eberli et al. 1993; Vecsei 1991; Morsilli et al. 2002; Rusciadelli 2005; Rusciadelli & Di Simone 2007 among others).

Between the middle and the late Cenomanian, the platform was once again submerged, leading to the recovery of shallow-water carbonate sedimentation (Vecsei et al. 1998; Rusciadelli & Di Simone 2007; Eberli et al. 2019). This resulted in the deposition of subtidal to supratidal limestones, rudist bioconstructions and bioclastic sand bodies of the Cima delle Murelle Formation (Rusciadelli & Di Simone 2007) (Fig. 1). These deposits concentrate in the central portion of the Maiella, along the platform margin. The inner platform is instead characterized by the Fondo di Maiella Formation, whereas pelagic, scaglia-like, facies developed to the south, representing the temporary drowning of the former platform deposits (Morsilli et al. 2002; Rusciadelli & Di Simone 2007). North of the platform escarpment the succession is mainly represented by base-of-slope deposits dominated by megabreccias and turbidites (Valle dell'Inferno and Tre Grotte formations; Fig. 1). All these formations collectively represent Supersequence 1 (SS1; sensu Vecsei 1991; Vecsei et al. 1998; Eberli et al. 2019) (Fig. 1).

The Cima delle Murelle, Fondo di Maiella, Valle dell'Inferno, and Tre Grotte formations are overlain by the Orfento Formation, spanning from the upper Campanian to the uppermost Maastrichtian and constituting Supersequence 2 (SS2; *sensu* Vecsei 1991, Vecsei et al. 1998; Eberli et al. 2019) (Fig. 1). The Orfento Formation marks the filling of the basin with the consequent shift in the large-scale stratigraphic architecture of the carbonate platform in the Maiella area from aggradation to progradation (Vecsei et al. 1998; Eberli et al. 2019). It consists of well-sorted bioclastic deposits, mass-transport deposits and limestone breccias. The coarse-grained bioclastic fraction is dominated by rudist debris associated with larger benthic foraminifera (LBF from here onward), sparse colonial corals, and calcareous red algae (Vecsei et al. 1998; Eberli et al. 2019). Small in-situ rudist bioconstructions and breccias with reworked rudists are also reported (Rusciadelli & Di Simone 2007).

The Orfento Formation is separated by the overlying Santo Spirito Formation by an erosive surface (Fig. 1). The Santo Spirito Formation itself is a complex unit of Paleogene age, consisting of various lithologies and including Supersequences 3, 4, 5 (SS3-5) (sensu Vecsei 1991; Vecsei et al. 1998; Eberli et al. 2019) (Fig. 1). The basal portion (corresponding to SS3) is the main focus of this research (Fig. 1C, E, F) and consists of turbidites, debris-flows, and other mass transport deposits of material that originated in the shallow-water areas of the platform, slumped downslope, and resedimented interbedded with pelagic limestones (Fig. 1) (Vecsei et al. 1998; Eberli et al. 2019). At the base large limestone blocks with a dominant boundstone texture have been reported. These large elements probably detached from the top of the platform during the Paleocene and have been originally attributed to two-time intervals: the Danian – early Selandian and the Selandian - early Thanetian (based on the data provided by Moussavian & Vecsei 1995 and recalibrated to the current biostratigraphic schemes of Schmitz et al. 2011; Wade et al. 2011; Serra-Kiel et al. 2020;

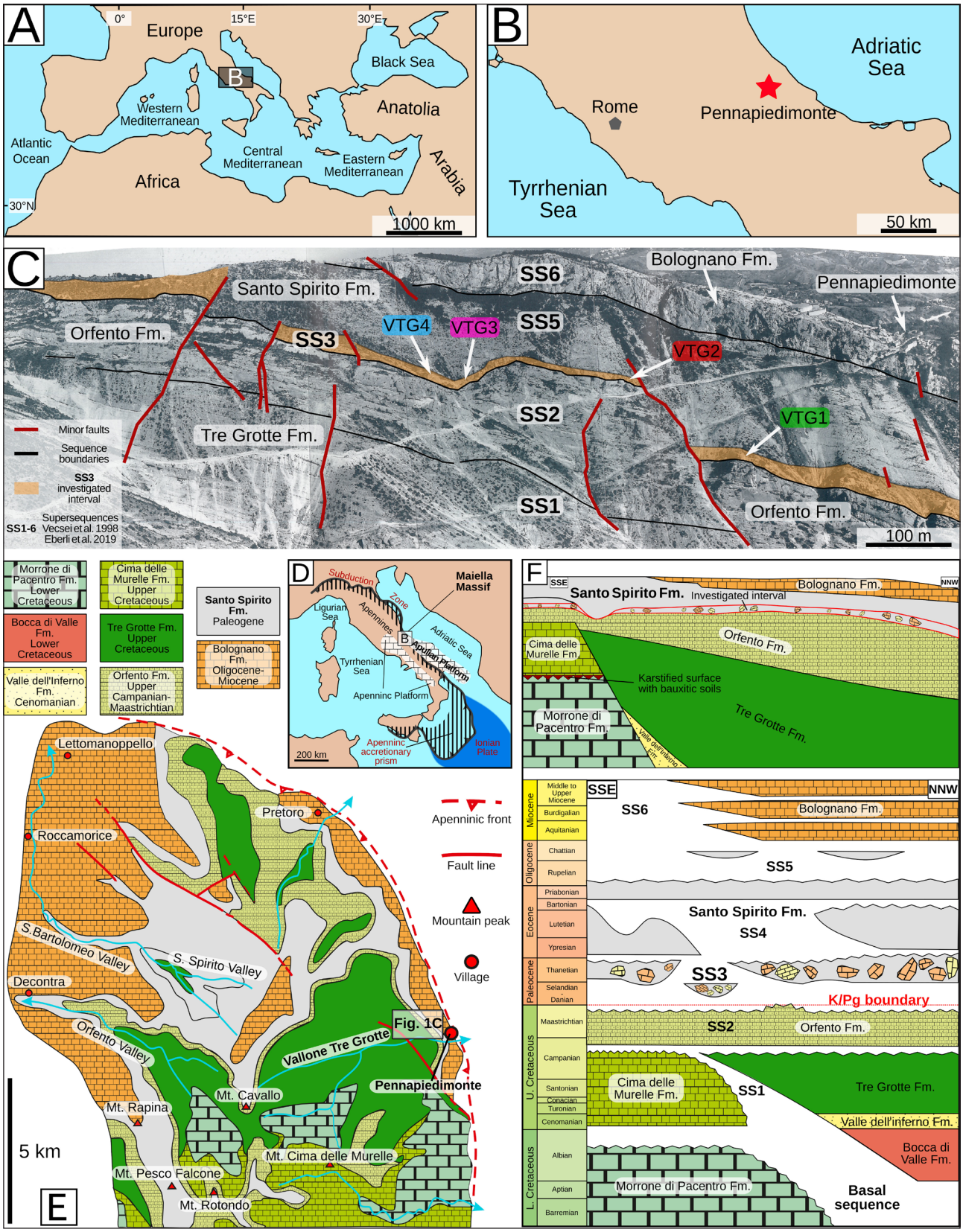

Fig. 1 - Geographic position and geological setting of the study area. A) The Mediterranean Sea. B) Central Italy. C) Sequence stratigraphic framework of the VTG, indicating the main sequences, highlighting the analyzed sequence (SS3) and the investigated outcrops, superimposed to the panoramic of the investigated area; modified from Vecsei (1991). D) Schematic geological map of Italy modified from Pomar et al. (2004) and Brandano et al. (2016b); the area covered by panel B is indicated by a gray box. E) Simplified geological map, with the main formations of the study area within the Maiella massif, modified from Vecsei & Sanders (1999) and Brandano et al. (2016b); the study area represented in Fig. 1C is indicated by a gray box. F) Schematic stratigraphic relationships, architecture and chronostratigraphic diagram of the Maiella platform margin modified from Eberli et al. (2019); supersequences (SS1-6) are described into the Geological Setting chapter, for further detail the reader is referred to Vecsei et al. (1998) and Eberli et al. (2019).

Papazzoni et al. 2023). The former group includes large-sized blocks (up to 400 m in length and 15 m in thickness), while the latter mainly includes boulder-sized elements (Moussavian & Vecsei 1995; Vecsei & Moussavian 1997). The blocks originally attributed to the Danian to early Selandian interval consist of boundstones with a framework built by a diverse assemblage of colonial corals and bound by calcareous red algae (Moussavian & Vecsei 1995; Vecsei & Moussavian 1997). Encrusting foraminifera and bryozoans also occur (Moussavian & Vecsei 1995; Vecsei & Moussavian 1997). The internal sediment of the bioconstructions is reported to be dominated by fragments of the bioconstruction itself, as well as by small benthic foraminifera (SBF) and calcareous green algae (Moussavian & Vecsei 1995; Vecsei & Moussavian 1997). No hyaline LBF indicative of late Thanetian age were reported (Shallow Benthic Zone 4 of Serra-Kiel et al. 1998, SBZ4) (Moussavian & Vecsei 1995; Vecsei & Moussavian 1997). The blocks originally attributed to the Selandian to early Thanetian interval include: boundstones dominated by encrusting corals and encrusting red calcareous algae; grainstones dominated by SBF (Moussavian & Vecsei 1995; Vecsei & Moussavian 1997). In both the internal sediment of the boundstones and in the associated grainstones, calcareous green algae, SBF and LBF are common (Moussavian & Vecsei 1995; Vecsei & Moussavian 1997). The latter include *Miscellanea* and *Ranikothalia* and an overall assemblage suggestive of a late Selandian to earliest Ypresian age (SBZ3 to SBZ5; Papazzoni et al. 2023) (Moussavian & Vecsei 1995; Vecsei & Moussavian 1997).

The lower (SS3) and middle (SS4) units of the Santo Spirito Formation (Fig. 1) are separated by a discontinuity surface displaying no clear evidence of subaerial exposure (Vecsei et al. 1998). The middle unit (Ypresian to lower Bartonian) consists of slope deposits with shallow-water material transported downslope, interbedded with pelagic limestones (Vecsei et al. 1998). The beds containing shallow-water allochems are often graded and mostly consist of LBF (nummulitids, orthophragmines, and alveolinids) associated with subordinated red calcareous algae and echinoderms (Vecsei et al. 1998). The upper boundary of this unit is represented by an erosive surface, possibly related to the exposure of the platform as suggested by the presence of *Microcodium* and microkarst in the downslope redeposited clasts (Vecsei et al. 1998).

The upper part of the Santo Spirito Formation (SS5) spans from the Bartonian to the late Rupelian (Fig. 1) (Vecsei & Moussavian 1997). This interval includes various types of mass transport deposits originating from shallow-water environments and redeposited in a slope setting (Vecsei et al. 1998). Among these, elements originating from the dismantling of coral bioconstructions of Rupelian age have also been reported (Vecsei et al. 1998). The upper boundary of the formation is represented by an erosive surface with evidence of subaerial exposure (Vecsei et al. 1998). Locally, small Rupelian coral bioconstructions have also been reported along this boundary (Vecsei et al. 1998).

The Santo Spirito Formation is overlain by the upper Chattian to lower Messinian Bolognano Formation (which represent SS6) (Fig. 1). The latter developed in a carbonate ramp environment, and consists of three shallow-water limestone units separated by deep-water marly limestones (Fig. 1) (Brandano et al. 2012, 2016a, b, 2020, 2022; Cornacchia et al. 2017).

Material and methods

The Maiella carbonate succession was investigated in the field along the northern flank of VTG, approximately 400 meters west of Pennapiedimonte (42.15°N, 14.18°E) (Fig. 2). The study area was chosen based on the maps, pictures, and interpretative schemes provided in Vecsei (1991), focusing in particular on the sections identified as "Avella SE", "Tre Grotte", "Avella E", "Avella W", and "Avella NW" (Fig. 1C). The limestone exposures located along these sections were initially observed using hand lenses to roughly assess their fossil content and to identify the basal breccia layer of the Santo Spirito Formation and the Paleocene blocks. Major structures and textures were also documented. Representative rock samples were collected right above the boundary between SS2 and SS3 and corresponding to the basal portion of the Santo Spirito Formation. Additional samples were collected also from the units above and below the investigated interval. Thin sections were prepared in the laboratory of the Department of Earth and Environmental Sciences of Milano-Bicocca University by G.C., M.A., and L.M. Rock samples were initially cut into hand-sized pieces and then consolidated through three embedding cycles with epoxy resin aimed at reinforcing the rock and filling both macroporosity and microporosity, resulting in high-quality thin sections preserving most of the morphological elements of the microfossils. After being polished with very-fine grained silicon carbide, the samples were glued to standard thin section glasses using UV-sensitive glue. Excess sample was removed using a Brumat thin-section saw and afterward the sections were further reduced to the desired thickness through hand-polishing, initially with a very-fine grained silicon carbide powder and then with aluminum oxide (grain size of 1 μm). Due to the highly lithified nature of the rock, hindering any effort at separating benthic foraminifera, serial thin sections of samples rich in foraminifera were produced for biostratigraphic purposes. With regards to stratigraphy, the capitalization of the names of

chronostratigraphic subdivisions of the Cenozoic follows Aubry et al. 2023. In total, 85 thin sections were prepared and examined through a Leica Leitz Laborlux S transmitted light optical microscope to identify components and rock textures for the subsequent microfacies description. All thin sections are stored in the Department of Earth and Environmental Sciences of the University of Milano-Bicocca. In 31 selected thin sections (the serial thin sections produced for biostratigraphic purposes were not selected for this analysis in order to not overestimate certain groups) microfacies characteristics were quantified using point-counting (Flügel 2010). For this analysis a 200 µm grid was utilized and more than 800 points were identified in each section.

Results

Description of the sections

Moving westward from the uppermost part of Pennapiedimonte village, various sections (VTG1-4), located at the boundary between the Orfento and Santo Spirito formations, have been analyzed (Fig. 2).

VTG1 (42.1517°N, 14.1895°E) is located below the main path and corresponds to section "Avella SE" as described by Vecsei (1991) (Figs. 2A, B; 3). The lower part of the section consists of a small crag situated near the edge of a cliff composed of Orfento Formation limestones (Fig. 3A) (Raffi et al. 2016: fig. 2). The uppermost layer of the Orfento Formation is represented by mudstones to wackestones dominated by silt-sized rudist fragments associated with common planktic foraminifera, such as globotruncanids (Fig. 3F-G). Sand-sized rudist fragments are generally concentrated in irregular patches separated by micrite-rich areas (Fig. 3F). This upper portion of the Orfento Formation is separated from the Santo Spirito Formation, constituting the small crag, by an erosive surface (Fig. 3A-E) (Vecsei 1991). The basal interval of the Santo Spirito Formation comprises clast-supported breccia characterized by pebble- to cobble-sized elements embedded in a fine-grained matrix (Fig. 3B-E). The clasts of the breccia consist of rudstones dominated by LBF, mainly *Siderolites* and *Orbitoides,* associated with common coral colonies and rudists (Fig. 3D, E, H-J). Towards the top of the crag, these clasts become less abundant. Microfacies analysis of the clasts of the breccia consistently indicates a Late Cretaceous age (see the chapter: Biostratigraphy). Around 30 m upwards (upper part of the section in Fig. 2A), the succession comprises fine-grained limestones interbedded with two normally-graded rudstone layers rich in nummulitids, orthophragmines, and coralline algae, suggesting an Eocene age (Fig. 3K).

VTG2 (42.1531°N, 14.1892°E) is located directly above the main path (Fig. 2A, C) between the upper part of the "Tre Grotte" section and the "Avella E" section as described by Vecsei (1991). Similarly to VTG1, VTG2 is situated at the boundary between the Orfento Formation and the Santo Spirito Formation (Fig. 4A). The Orfento Formation is well exposed along the road cut of the main path (lower part of the section VTG2 in Fig. 2A), where large blocks (up to 1 m in diameter) of rudist-dominated floatstone to rudstone are present (Fig. 4B, C). These coarse-grained blocks are embedded within a mudstone matrix rich in planktic foraminifera, such as globotruncanids (Fig. 4D). Granule- and fine-pebble-sized intraclasts of planktic foraminiferal mudstone can be observed at the boundary between the rudist-dominated floatstone to rudstone and the embedding mudstone (Fig. 4E, F). The uppermost part of the Orfento Formation mainly consists of mudstone to wackestone with a sparse bioclastic fraction, including Late Cretaceous LBF and globotruncanids (Fig. 4G). The basal portion of the overlying Santo Spirito Formation consists of 10 m of massive floatstone to rudstone exhibiting pebble- to cobble-sized elements embedded within a wackestone matrix (upper part of VTG2 in Fig. 2A). However, the outcrop surface is considerably altered, making it impossible to accurately describe the large-scale texture (Fig. 2C). Some clasts include relatively complete rudist specimens whereas other clasts mostly consist of coral colonies. All but one of the pebble- and cobble-sized clasts are characterized by Upper Cretaceous LBF (Fig. 4H). The only exception is represented by a bindstone sample dominated by encrusting corals and red calcareous algae (Fig. 4I), which does not include any diagnostic elements of either Late Cretaceous or Eocene age. The massive floatstone to rudstone layer is overlain by a mudstone with planktic foraminifera, possibly acarinids or morozovellids (Fig. 4J).

VTG3 is located further westward above the main path (42.1543°N, 14.1868°E) (Fig. 2A, D). It roughly corresponds to the section "Avella W" as described by Vecsei and Moussavian (1997). Similar to VTG1 and VTG2, it is situated atop of an erosional surface that separates the underlying Orfento Formation from the overlying Santo Spirito Formation (Figs. 2D; 5A). Directly above this surface, cobble- to boulder-sized blocks of coral-boundstone

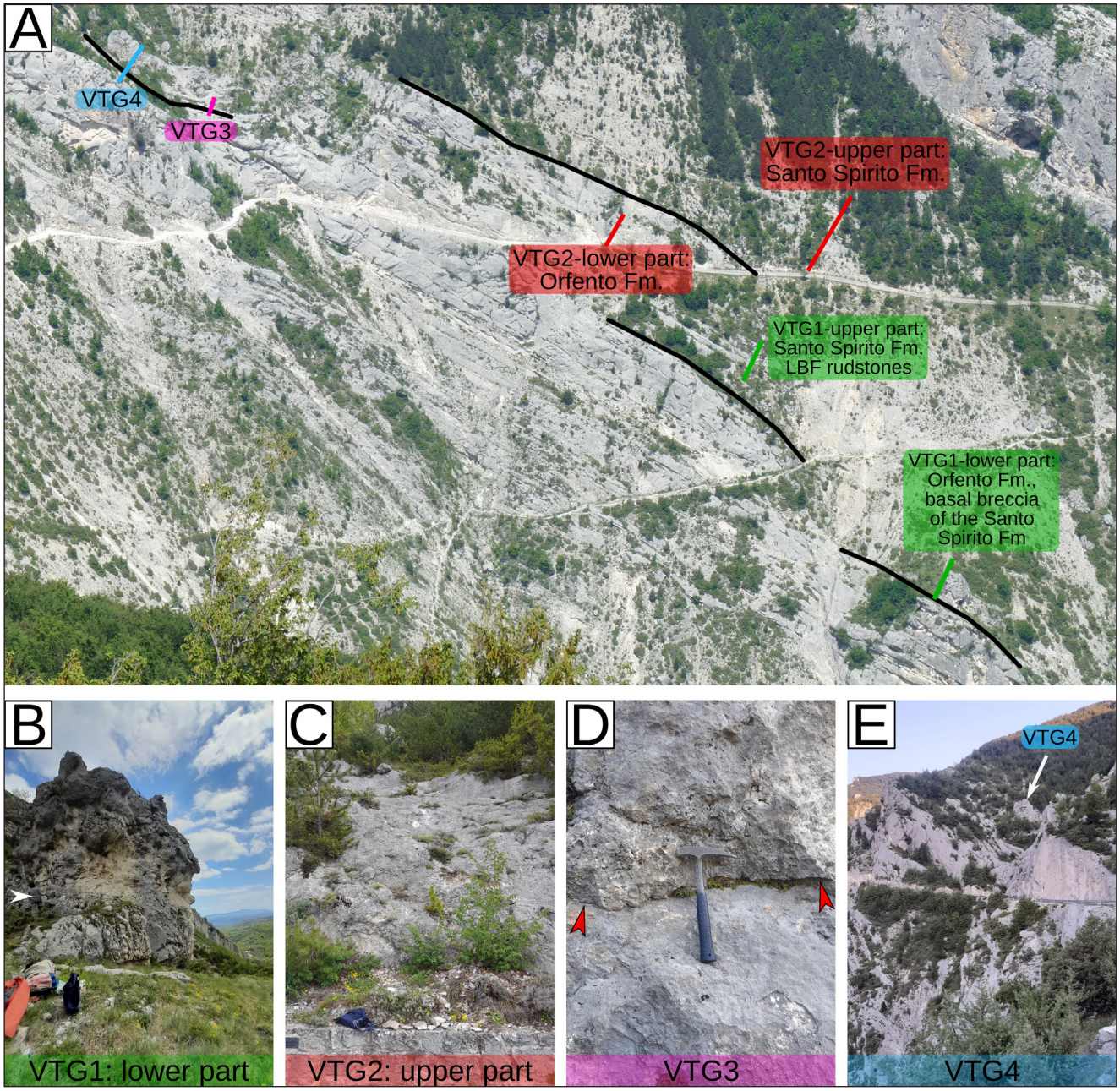

Fig. 2 - The investigated VTG sections near Pennapiedimonte. A) Panoramic picture of the investigated area taken from the other side of VTG. B) Basal breccia of the Santo Spirito Formation overlying the Orfento Formation at VTG1; white arrowhead indicates a person for scale. C) Basal breccia of the Santo Spirito Formation overlying the Orfento Formation at VTG2 as seen from the main path of the VTG. D) Boundary between the Orfento Formation (SS2) and Santo Spirito Formation (SS3) at VTG3, red arrowhead indicates the discontinuity surface. E) Panoramic view of the VTG4 outcrop.

can be observed (Fig. 5B-H). The corals are moderately well preserved, and it is possible to observe the framework of the boundstone consisting of coral colonies encrusted by secondary binders (Fig. 5B-H). Coral colonies display massive, encrusting and branching (mainly phaceloid colonies) growth forms (Fig. 5B-D). Secondary binders are mainly represented by calcareous red algae and encrusting foraminifera (Fig. 5E-H). Patches of poorly sorted bioclastic material (floatstone to wackestone) can be observed trapped between coral colonies (Fig. 5C). The micropaleontological analysis (see the chapter Biostratigraphy) indicates a Paleocene age. Differently from the description of Vecsei & Moussavian (1997), these boundstone clasts are rather sparse and appear to be embedded within a fine-grained matrix that also includes reworked Late Cretaceous LBF.

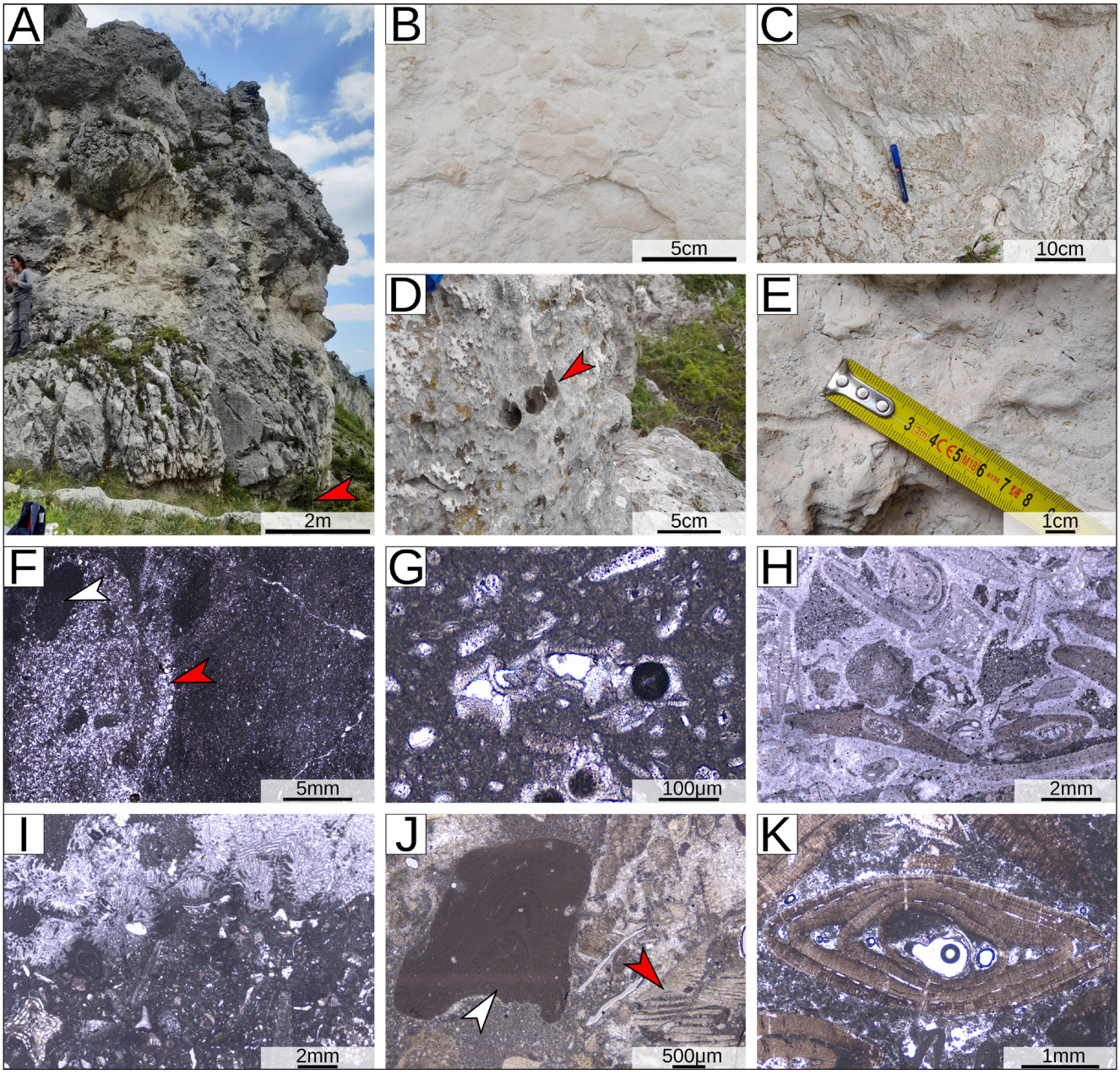

Fig. 3 - VTG1. A) Overview of the outcrop; red arrowhead indicates the boundary with the underlying Orfento Formation. B) Clast-supported breccia at the base of the Santo Spirito Formation. C) Cobble sized clast of LBF rudstone in the clast-supported breccia at VTG1. D) Rudist specimens (red arrowhead). E) Rudist specimens displaying the inner structures of their shells. F) Mudstone to wackestone with rudist fragments that constitute the uppermost part of the Orfento Formation, most of the fragments are silt-sized (as in the pictured example), locally larger fragments also occur; red arrowhead indicates a patch packed with silt-sized rudist fragments; white arrowhead= mudstone intraclast within the patch rich of rudist fragments denoting the pervasive mixing of different assemblages in the upper part of the Orfento Formation. G) Globotruncanid from the mudstone to wackestone of the uppermost Orfento Formation. H) Thin section of a LBF rudstone cobble from the clast supported breccia of the Santo Spirito Formation. I) LBF rudstone cobble rich in fragments of colonial corals. J) LBF rudstone with coralline algae (white arrowhead) and rudist fragments (red arrowhead). K) Thin section from the LBF rich rudstone located around 30 m above the basal breccia of the Santo Spirito Formation at VTG1 and displaying the detail of a pseudo-axial sections of *Nummulites*.

VTG4 is located further westward (42.1542°N, 14.1862°E), roughly corresponding to the section "Avella NW" as described by Vecsei and Moussavian (1997) (Fig. 2A, E). It consists of a roughly 10 m high cliff of coral-boundstone (Figs. 2A, E; 6A). The outcrop does not display a significant lateral continuity and appears to extent only a few tens of meters over the surface separating the Orfento and Santo Spirito formations. The boundstone displays a wide variety of coral growth forms, including encrusting colonies and several types of domal and branching forms (Fig. 6B-E). The micropaleonto-

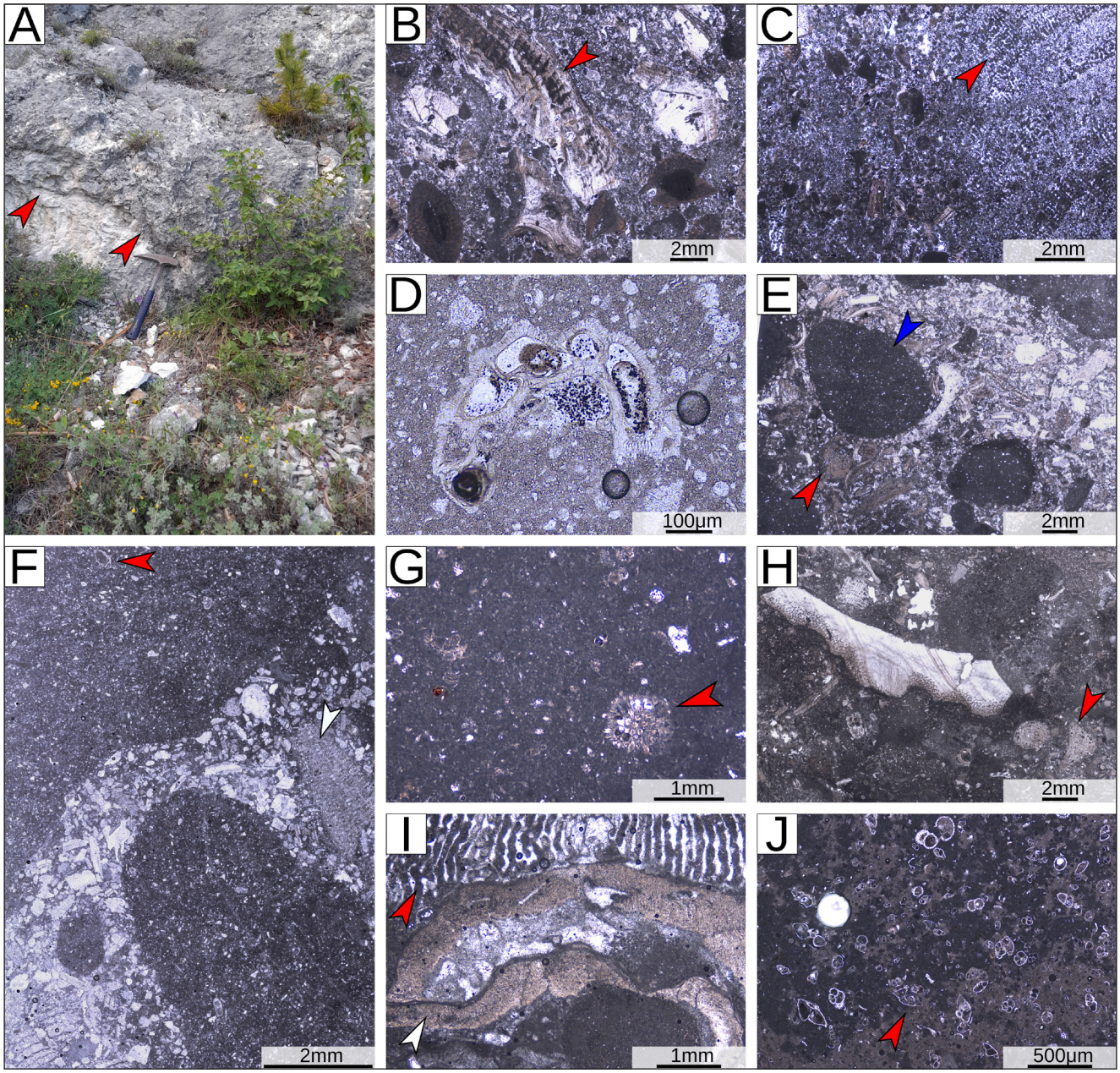

Fig. 4 - VTG2. A) Boundary with the underlying Orfento Formation (red arrowheads). B) Thin section from one of a boulder of rudist-dominated rudstone to floatstone from the upper Orfento Formation, displaying a skeletal assemblage dominated by rudist fragments and LBF. C) Thin section of an other boulder of rudstone to floatstone of the upper Orfento Formation characterized by abundant fragments of colonial corals displaying evidence of partial dissolution. D) Globotruncanid within the mudstone embedding the rudist-dominated rudstone to floatstone. E) Lower portion of the section with granule-sized intraclasts of mudstone (blue arrowhead) at the boundary between the rudist-dominated rudstone to floatstone and the embedding mudstone with planktic foraminifera; red arrowhead indicates a *Siderolites* specimen within the coarse-grained bioclastic sediment dominated by rudist fragments. F) Detail of planktic foraminifera mudstone intraclasts at the boundary with the rudist-dominated rudstone to floatstone in the Orfento Formation at VTG2; red arrowhead indicates a globotruncanid within the mudstone; white arrowhead indicates an *Orbitoides* within the rudstone. G) Mudstone to wackestone with scattered LBF in the uppermost Orfento Formation; red arrowhead indicates a *Siderolites* specimen. H) Rudist and LBF within the massive floatstone to rudstone at the base of the Santo Spirito Formation; red arrowhead indicates a *Siderolites* specimen. I) Bindstone clast sampled from the basal massive floatstone to rudstone of the Santo Spirito Formation, differently from the other analyzed clasts it lacks typical Late Cretaceous elements; red arrowhead indicates a colonial coral; white arrowhead indicates a red calcareous alga. J) Upper part of VTG2 section, characterized by planktic foramifera mudstone with possible morozovellids (red arrowhead) and acarinids.

logical analysis of samples from the coral boundstone of VTG4 (see the chapter Biostratigraphy) indicates a Paleocene age.

Biostratigraphy

The mudstones and wackstones of the uppermost Orfento Formation at VTG1 and VTG2

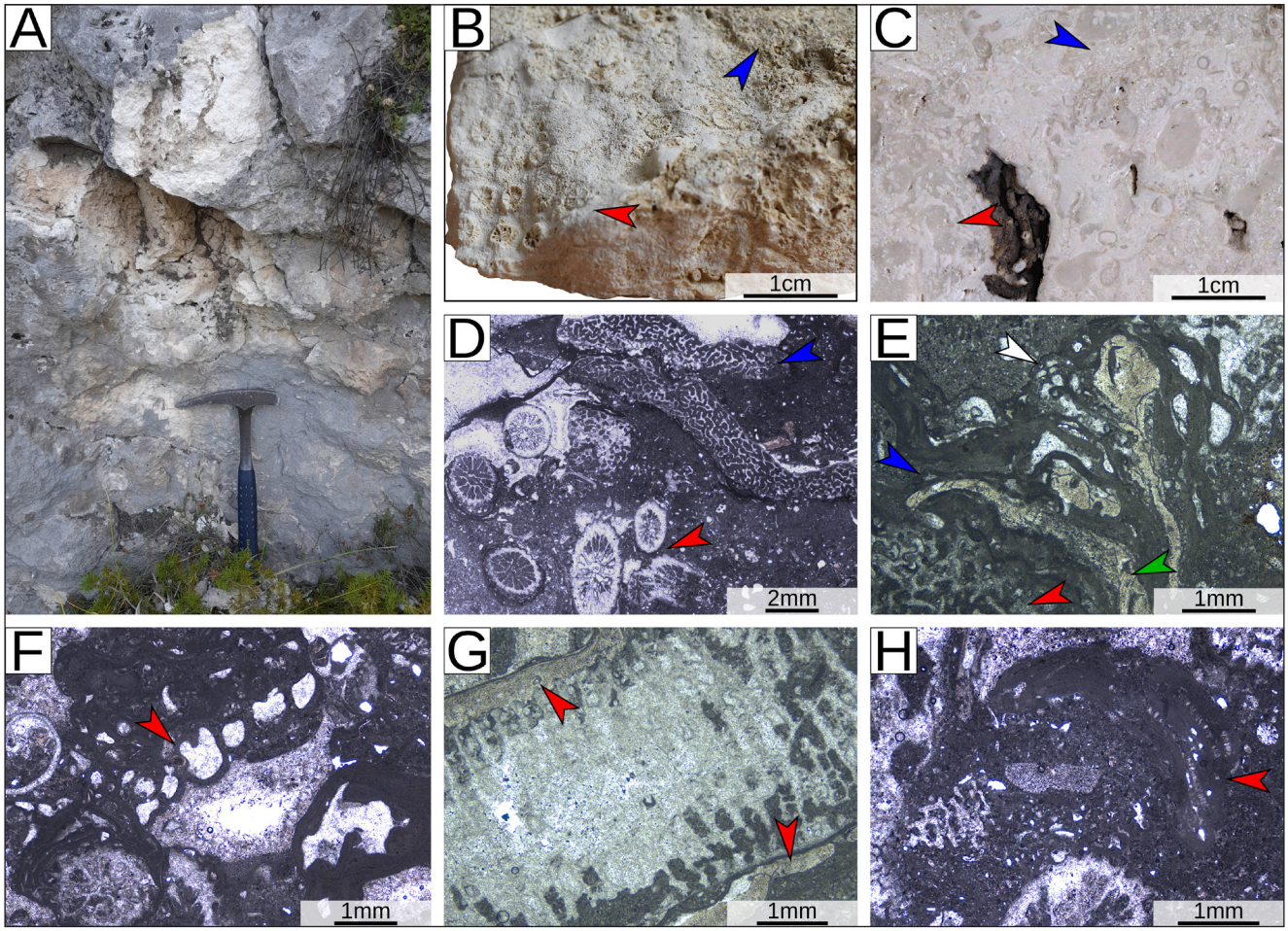

Fig. 5 - VTG3. A) Coral boundstone boulder. B) Detail of a slab cut from the coral boundstone boulder. C) Polished lower surface of the slab in panel B; red arrowhead indicates the corallites of a coral colony; blue arrowhead indicates a patch of poorly sorted sediment trapped between coral colonies. D) Thin section from the coral boundstone displaying different coral morphologies; red arrowhead indicates branching, phaceloid, colonial corals; blue arrowhead indicates platy/encrusting colonial corals. E) Colonial coral (red arrowhead) encrusted by Peyssonneliales algae (green arrowhead), coralline algae of the order Corallinales (blue arrowhead), and agglutinated encrusting benthic foraminifera (white arrowhead). F) Agglutinated encrusting benthic foraminifera (red arrowhead). G) Colonial coral encrusted by Peyssonneliales red calcareous algae (red arrowheads). H) Molds of a colonial coral encrusted by a Sporolithales red calcareous alga (red arrowheads).

are rich in globotruncanids, suggesting a Late Cretaceous age (Sartorio & Venturini 1988) (Figs. 3G; 4D). This is consistent with magnetostratigraphic and biostratigraphic data that place the uppermost part of the Orfento Formation at Pennapiedimonte in the upper Maastrichtian (Lampert et al. 1997; Eberli et al. 2019).

The floatstone to rudstone blocks embedded within the mudstone of the Orfento Formation at VTG2, include common specimens of *Orbitoides* sp., *Siderolites calcitrapoides* (Lamarck 1801) (Fig. 4F, G), supporting a Maastrichtian age (Sartorio & Venturini 1988; Chiocchini & Mancinelli 2001; Robles-Salcedo et al. 2018; Benedetti 2019; Özcan et al. 2021; Vicedo & Robles-Salcedo 2022). Similarly, the clasts of LBF rudstone observed at VTG1, based on the presence of *Orbitoides*, *Simplorbites*, *Hellenocyclina beotica* (Reichel 1949), *Siderolites calcitrapoides*, and *Omphalocyclus macroporus* (Lamarck 1816) (Fig. 7A-C), are also of Maastrichtian age. Late Cretaceous LBF assemblages were also observed in the clasts of the massive floatstone to rudstone layer constituting the base of the Santo Spirito Formation at VTG2 (Fig. 4H).

The coral-boundstones of VTG3 and VTG4 are also located in the basal layer of the Santo Spirito Formation, right above the discontinuity surface that separates the latter from the underlying upper Maastrichtian Orfento Formation. Around 30 meters above the investigated basal breccia of the Santo Spirito Formation rudstone layers characterized by Eocene LBF taxa have been recorded in the

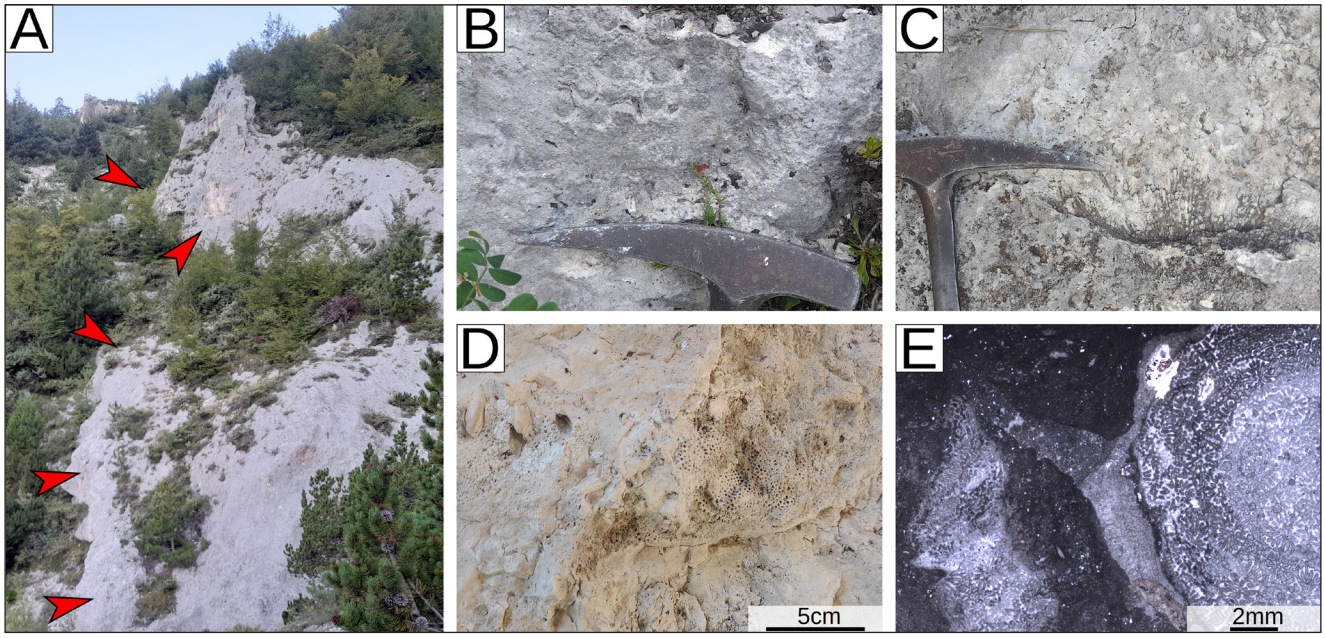

Fig. 6 - VTG4. A) Overview of the cliff of Paleocene coral boundstone with red arrowheads indicating sampling sites. B) Domal colony with large corallites. C) Domal colony. D) Encrusting/domal massive plocoid colony with small corallites, possibly comparable to the genus *Actinacis* (sensu Bosellini & Russo 1995). E) Thin section with colonial corals (possibly comparable to genus *Actinacis*) embedded in a micritic matrix.

current analysis (Fig. 2A). Previous researches in the VTG have constrained, using calcareous nannofossils, the lower part of the Santo Spirito Formation, above the basal breccia, within Lutetian (Raffi et al. 2016), whereas in the nearby Orfento Valley (Fig. 1E) the base of the formation has been constrained to the Selandian - early Thanetian (Cornacchia et al. 2018). The coral-boundstones of VTG3 and VTG4 must have thus formed between the Maastrichtian and the Middle Eocene. The benthic foraminiferal assemblage of the boundstones is quite scarce and consists of small taxa characterized by a simple structure. Some of the observed individuals could be tentatively attributed, given the small size of the test and the diameter of the proloculus, to *Planorbulina antiqua* (Mangin 1960) (Fig. 7D, E). This species has a proloculus ranging in diameter between 40 and 60 µm (differently from the larger *Planorbulina cretae* Marsson 1878) and is recorded from the Maastrichtian to SBZ2 (Serra-Kiel et al. 2020). Other specimens bear some resemblance to Lower Paleocene members of the genera *Valvulineria* and *Cocoarota* (Consorti & Köroğlu 2019; Consorti & Schlagintweit 2022; Serra-Kiel et al. 2020; Papazzoni et al. 2023) (Fig. 7F). Genera like *Miscellanea* and *Ranikothalia*, reported and depicted by Moussavian & Vecsei (1995) were not observed notwithstanding the large number of thin sections produced from samples rich in benthic foraminifera. Likewise, no other genera clearly diagnostic of a Selandian or Thanetian age were observed. The boundstones of VTG3 and VTG4 include a relatively wide variety of calcareous green algae (Fig. 7G-M). Although most of the specimens are poorly preserved, some individuals could be tentatively identified as *Microsporangiella* cf. *buseri* (Barattolo 1998) (Fig. 7G). *Microsporangiella buseri* has been reported by Barattolo (1998) in Slovenian limestones attributed to SBZ1 and commonly occur in lower Danian lagoonal sediments from the Pyrenees. Other algae could be tentatively attributed to the genera *Orioporella*, *Clypeina*, and *Cymopolia* (Fig. 7H-K). Based on the similarities with the green algal assemblages investigated by Barattolo (1998) in Slovenia and northeastern Italy, the investigated coral bioconstructions should have developed during an interval spanning from SBZ1 to SBZ3, thus encompassing the Danian, the Selandian and the early Thanetian (Serra-Kiel et al. 1998, 2020; Papazzoni et al. 2023). Given the presence of *Microsporangiella* cf. *buseri*, and of *Planorbulina antiqua*, the boundstone of VTG3 and VTG4, most likely, developed during the early Danian (Barattolo 1998; Serra-Kiel et al. 2020). This hypothesis is in agreement with all the existing literature on this

unit (Moussavian & Vecsei 1995; Vecsei & Moussavian 1997; Vecsei et al. 1998; Eberli et al. 2019). No evidence for a different placement has emerged notwithstanding the large number of produced thin sections that highlighted (within the margin of the reasonable doubt) the lack of Upper Cretaceous LBF assemblages (which are instead largely common in the units mere meters below the investigated boundstone), Eocene LBF assemblages (which are largely common in the layers above the investigated boundstone), and Thanetian LBF (which have been reported in the overlying shallow-water limestone blocks reported by Moussavian & Vecsei 1995). LBF were particularly affected by the end-Cretaceous mass extinction, few genera passed the K/Pg boundary and, with the exception of *Laffitteina,* only taxa with small and simple tests are generally recorded in the lower Danian (Inan et al. 2005; Drobne et al. 2007; Serra-Kiel et al. 2020; Bendetti & Papazzoni 2022). Rotaliids significantly diversified only from the late Danian onward (SBZ2) (Benedetti & Papazzoni 2022; Sinanoğlu et al. 2022). As a result of that, lower Danian communities (SBZ1) are defined by poorly diversified assemblages occurring between the extinction of Upper Cretaceous fauna and the first appearance of the earliest Cenozoic taxa characterized by a complex structure (e.g., *Kayseriella decastroi* Sirel, 1999, *Elazigina dienii* Hottinger, 2014, miscellaneidae) (Sinanoğlu et al. 2022; Papazzoni et al. 2023). *Bangiana hanseni* (Drobne, Ogorelec & Riccamboni 2007) is one of the few species generally considered suggestive of SBZ1 (Drobne et al. 2007). However, since it is usually associated with very shallow and restricted environments (Drobne et al. 2007), its absence in the investigated assemblages might be related to environmental reasons. *Laffitteina*, one of the few survivors of the end-Cretaceous extinction, has been reported in the lower Danian of Turkey (Inan et al. 2005), but it is absent in the lower Danian of northern Italy and Spain (Serra-Kiel et al. 2020; Papazzoni et al. 2023), indicating that it was not common throughout Tethys during the early Danian. Consequently, although not diagnostic in and of itself, the low-diversity foraminiferal assemblage of VTG3 and VTG4, which entirely lacks complex forms and includes *Planorbulina antiqua*, would be poorly compatible with a placement other than the early Danian (a placement which is also in agreement with the green calcareous algal assemblage).

Skeletal assemblage and microfacies

As already noted by previous authors based on the chaotic nature of the boundstone blocks, the presence of breccia layers, and the presence of channels and erosive surfaces (Moussavian & Vecsei 1995; Vecsei & Moussavian 1997; Vecsei et al. 1998; Raffi et al. 2016; Eberli et al. 2019), the investigated interval of the VTG succession, spanning the uppermost Orfento Formation and lowermost Santo Spirito Formation, displays clear evidence of reworking of shallow-water material. The latter was transported downslope and mixed with deep-water material (outer-ramp or slope deposits) (e.g., Figs 4E, F). However, the LBF rudstone clasts at VTG1 (Fig. 3B, C), the boulders of rudist floatstone to rudstone at VTG2 (Fig. 4B, C), and the coral boundstones at VTG3 and VTG4 (Figs. 5; 6) represent resedimented elements with their own internal consistency and without clear evidence of mixing of heterogeneous assemblages. Therefore, they can provide information on the environment where they developed (Schlager 1991; Schlager et al. 1996; Coletti et al., 2015, 2016; Buček & Köhler 2017) and thus a detailed microfacies analysis was performed on them (Tab. 1).

The skeletal assemblage of the upper Maastrichtian pebbles and cobbles of LBF rudstone, reworked in the basal breccia of the Paleogene Santo

Fig. 7 - Age diagnostic microfossils of the investigated outcrops. A) *Siderolites calcitrapoides* from the LBF rudstone clast of the clast-supported Breccia at the base of the Santo Spirito Formation at VTG1. B) *Omphalocyclus macroporus* from the LBF rudstone clast of the clast-supported breccia at the base of the Santo Spirito Formation at VTG1. C) *Orbitoides* sp. from the LBF rudstone clast of the clast-supported breccia at the base of the Santo Spirito Formation at VTG1. D) VTG3, *Planorbulina antiqua*, red arrowhead indicates the proloculus. E) VTG4, axial section *Planorbulina antiqua* growing over a specimen of a red calcareous alga of the order Peyssoneliales (red arrowhead). F) VTG3, poorly oriented section possible belonging to a specimen of *Valvulineria patalaensis*. G) *Microsporangiella* cf. *buseri* from the coral boundstone of the Santo Spirito Formation at VTG4. H) *Clypeina* cf. *socaensis* from the coral boundstone of the Santo Spirito Formation at VTG4. I) *Clypeina* sp. from the coral boundstone of the Santo Spirito Formation at VTG4. J) *Orioporella* sp. from the coral boundstone of the Santo Spirito Formation at VTG4. K) Axial cut of an element of a *Cymopolia* sp., from the coral boundstone of the Santo Spirito Formation at VTG4. L) Coral boundstones of VTG3, poorly diagnostic sub-transverse cut of an element of a green calcareous alga, vaguely resembling some specimens of *Acroporella chiapasis* (Deloffre, Fourcade & Michaud 1985) reported by Barattolo (1998) from the Danian of Slovenia. M) Poorly diagnostic sub-transverse cuts of green algal specimens from the coral boundstone of the Santo Spirito Formation at VTG4.

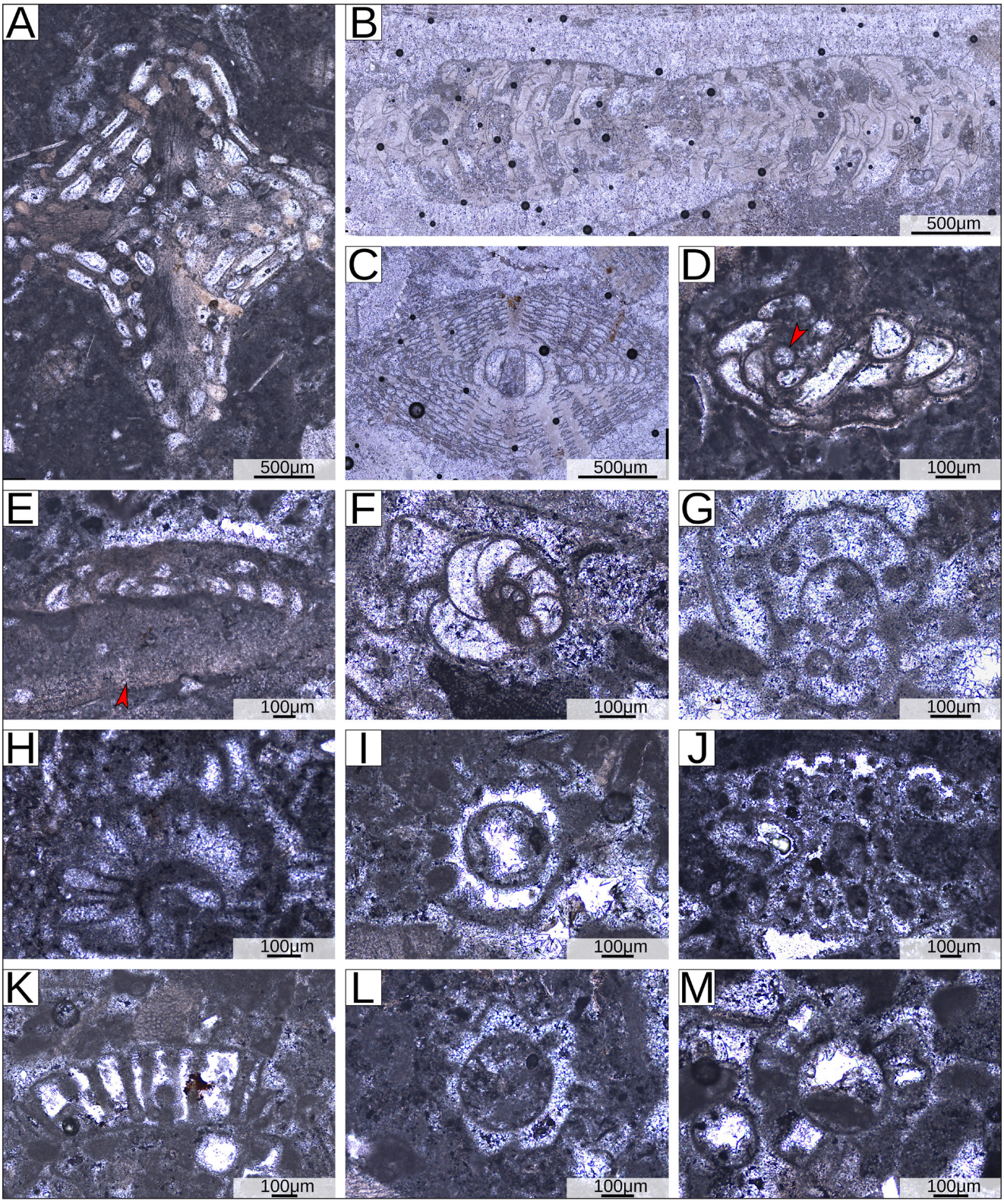

Fig. 7

Spirito Formation at VTG1, is dominated by hyaline LBF (53.5%; mainly *Orbitoides* and *Siderolites*), associated with common rudists (18%; mainly fragments but also whole specimens) (Fig. 8A-C), and colonial corals (13%; Tab. 1) (Fig. 8B, D). Echinoderms (Fig. 8C), encrusting benthic foraminifera (mainly hyaline taxa) (Fig. 8D), SBF (mainly hyaline), and red calcareous algae also occur. Bryozoans are rare.

Skeletal grains are relatively well-sorted and the space between them is filled by significant amounts of micrite and sparite (Fig. 8E). Peloids also occur locally, but overall they are rare.

The upper Maastrichtian floatstone to rudstone blocks observed in the upper part of the Orfento Formation at VTG2 are dominated by rudists (46%; Tab. 1), both complete specimens and small angular fragments (Fig. 8F). The rudists are associated with abundant colonial corals (34.5%; Tab. 1) displaying extensive evidence of recrystallization (Fig. 8G). LBF are also common (9%; mainly *Orbitoides*, but *Siderolites* also occurs) (Fig. 8G). Encrusting benthic hyaline foraminifera are often observed on large-sized skeletal grains (Fig. 8G). Echinoderms and SBF (mainly hyaline taxa) are rare, whereas red calcareous algae are very rare. Peloids are also rare. The clasts are embedded into a relatively well-sorted fine-sand sized matrix (possibly resulting from the fragmentation of rudist shells and non-skeletal grains) which often displays evidence of recrystallization.

The skeletal assemblages of the lower Danian coral boundstones of VTG3 and VTG4 are largely dominated by colonial corals (65-66%; Tab. 1). The corals are associated with common calcareous red algae (22-24%), which usually bind corals together (Figs. 5C-H; 8H, I). The calcareous red algal assemblage is dominated by Peyssonneliales and Sporolithales (Figs. 5G, E, H; 8J-M). Among the former most of the specimens display morphological features very different from those of some of their modern relatives such as *Polystrata* (Kato et al. 2006; Pestana et al. 2021) (Fig. 8J, K). Rare *Karpathia* (Fig. 8L) and very rare Hapalidiales (Fig. 8M) and Corallinales are also present. The frame of the boundstone also includes a significant amount of encrusting benthic foraminifera, mainly agglutinated taxa (e.g., Fig. 5F), but also miliolids and rotaliids. The sediment trapped within the small cavities of the frame is poorly sorted and mainly consists of micrite, associated with small peloids and some skeletal grains (Fig. 8H, I, N, O). The latter include SBF (both hyaline and porcelaneous taxa), calcareous green algae, bryozoans, mollusks, echinoderms, and ostracods. The main difference between VTG4 and VTG3 is that small peloids are more common in VTG4 than in VTG3, and that in VTG4 the micritic matrix that fills most of the space of the bioconstructions can locally display irregular lamination, possibly suggestive of a microbial origin.

Discussion

The various investigated blocks of shallow-water limestone of Late Cretaceous and Danian age clearly represent reworked elements transported downslope into more fine-grained sediments. This is testified by the stark contrast between the assemblage of these limestone blocks, dominated by carbonate producers typical of the photic zone, and the surrounding fine-grained sediments rich in bioclasts of the pelagic domain (e.g., Fig. 4E, F). This contrast is especially clear in the basal layer of the Santo Spirito Formation. At VTG1 the clasts of Upper Cretaceous shallow water limestone are concentrated right above a major unconformity surface, and they are embedded into fine-grained pelagic sediments that, slightly above the top of VTG1 section, have been dated to the Eocene based on calcareous nannoplankton (Raffi et al. 2016). This is in overall agreement with previous researches that, according to sedimentary structures, erosive sur-

Fig. 8 - Microfacies of the analyzed succession. A) LBF rudstone from VTG1; red arrowhead indicates the porosity resulting from the dissolution of a small bivalve; blue arrowhead indicates a specimen of *Simplorbites*; green arrowhead indicates *Hellenocyclina beotica*. B) LBF rudstone from VTG1; red arrowheads indicate coral fragments; blue arrowhead indicates a rudist fragment. C) LBF rudstone from VTG1; red arrowhead indicates an echinoderm fragment. D) LBF rudstone from VTG1 displaying a colonial coral encrusted by an acervulinid hyaline encrusting benthic foraminifer= red arrowheads. E) LBF rudstone from VTG; red arrowhead indicates sparry calcitic cement. F) Rudist-dominated rudstone to floatstone from VTG2; red arrowheads indicate rudist fragments. G) Rudist-dominated rudstone to floatstone from VTG2; red arrowheads indicate partially recrystallized fragments of colonial corals; blue arrowhead indicates an encrusted foraminifera growing over a fragment of a colonial coral; white arrowhead indicates a specimen of *Siderolites*. H) Coral boundstone from VTG3; red arrowhead indicates a gastropod. I) Coral boundstone from VTG3, red arrowhead indicates encrusting coralline algae biding corals together; white arrowheads indicate micrite filling the spaces within the frame. J) Red calcareous alga of the order Peyssonneliales from the coral boundstone of VTG4. K) Red calcareous alga of the order Peyssonneliales from the coral boundstone of VTG3. L) *Karpathia* from the coral boundstone of VTG4. M) Coralline algae from the coral boundstone of VTG3; red arrowhead indicates a specimen of coralline alga of the order Hapalidiales; white arrowhead indicates a specimen of coralline alga of the order Sporolithales; blue arrowhead indicates an echinoderm spine. N) Bioclastic sediment occurring within the colonies of the coral boundstone of VTG3; red arrowhead indicates a bryozoan. O) Bioclastic sediment occurring within the colonies of the coral boundstone of VTG4; red arrowheads indicate a small agglutinated benthic foraminifer; white arrowhead indicates a small miliolid; blue arrowheads indicate fragments of a green calcareous alga.

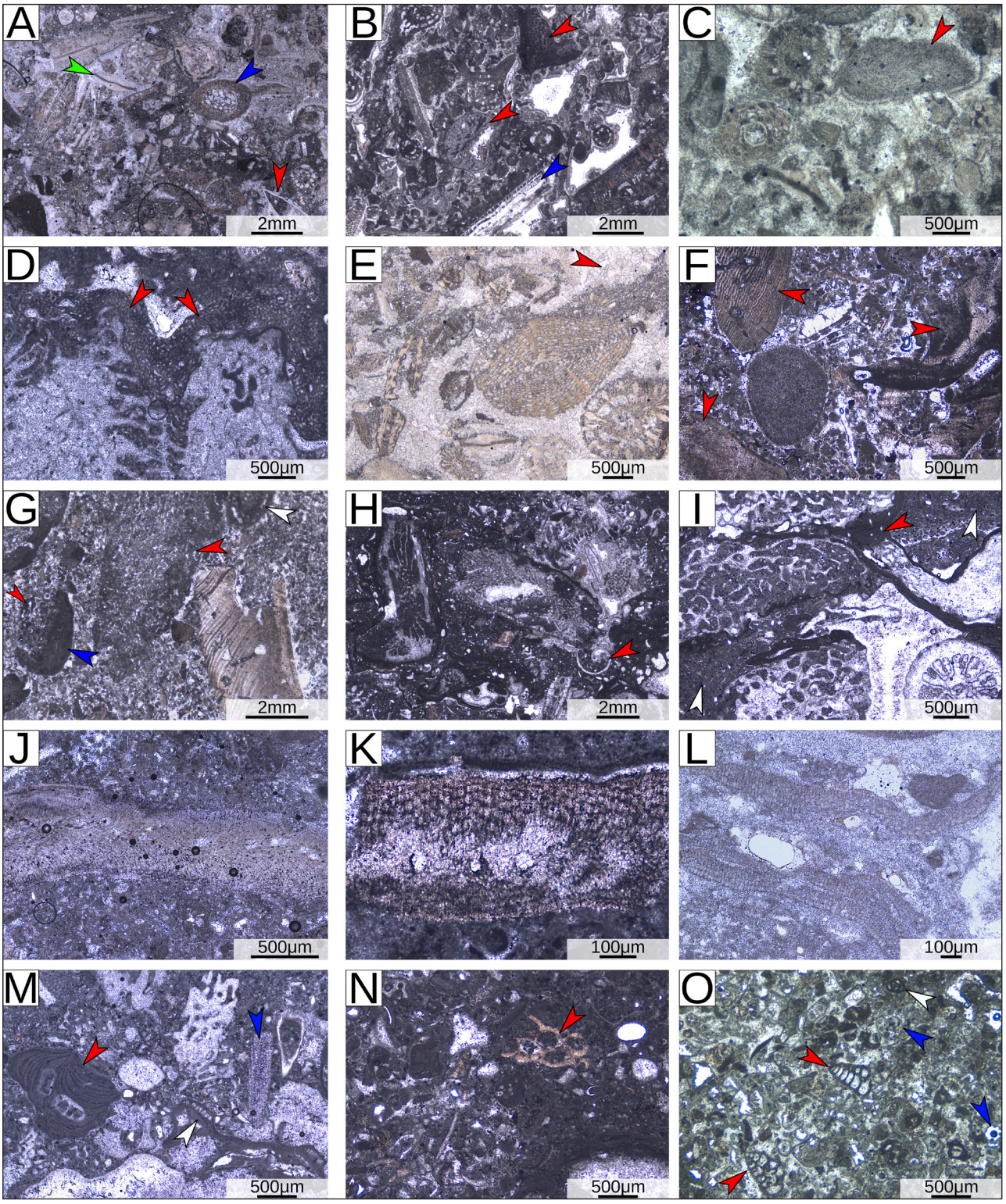

Fig. 8

faces, the characteristics of the basal breccia layer, and micropaleontological evidence, interpreted the Santo Spirito Formation as an outer-ramp deposit fed by both pelagic rain and shallow-water material transported downslope (Moussavian & Vecsei 1995; Vecsei & Moussavian 1997; Vecsei et al. 1998; Eberli et al. 2019). Following this assumption and combining the stratigraphic sections of Vecsei (1991) and Vecsei and Moussavian (1997) with the results of the current research, an idealized combined stratigraphic log of the area of the VTG near Pennapiedimonte can be drafted (Figs. 2; 9). The latter illustrates the great lithological variability of the basal breccia of the Santo Spirito Formation,

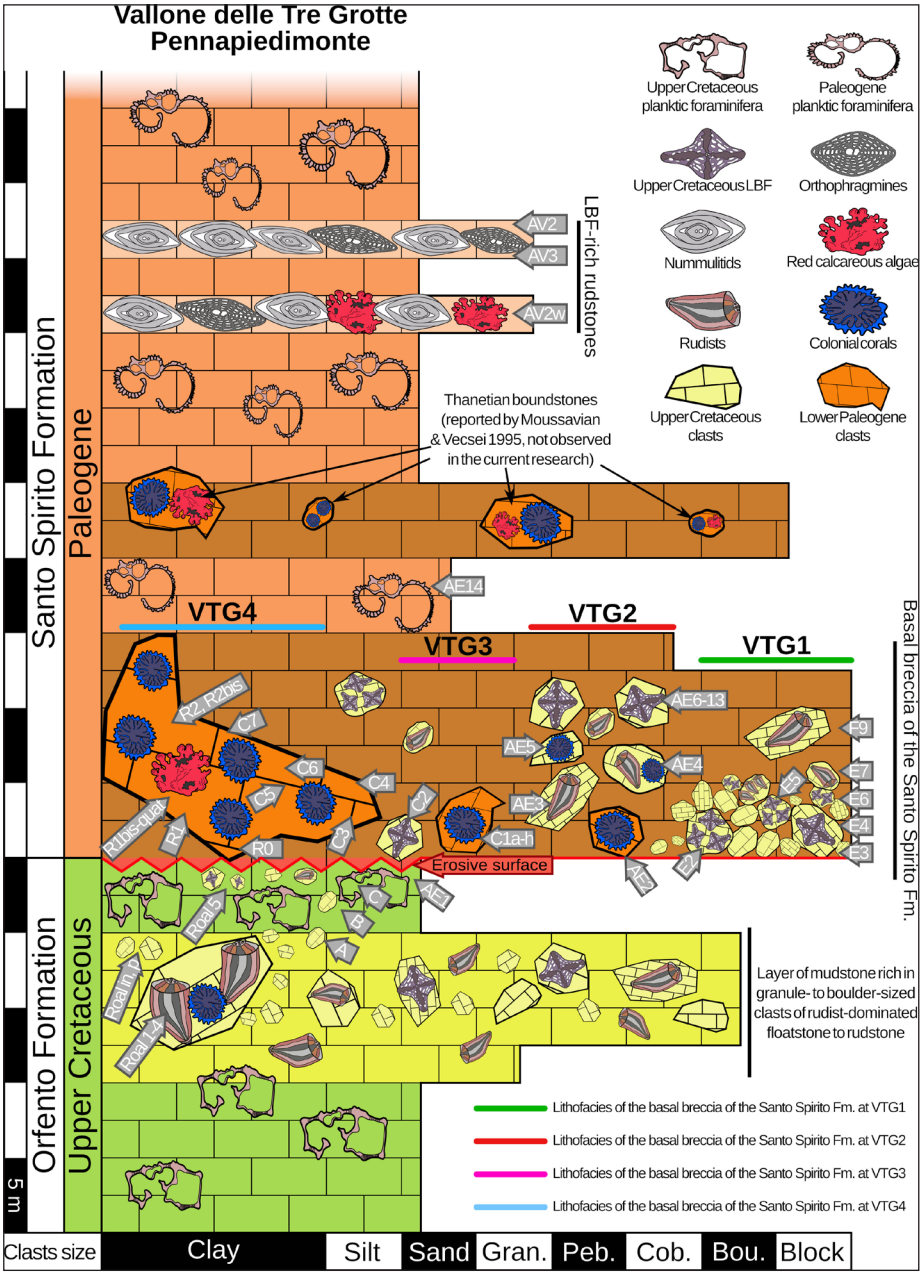

Fig. 9 - Idealized interpretative stratigraphic log of the area of the VTG near Pennapiedimonte that incorporates field data from the examination of VTG1-4 with the stratigraphic sections of Vecsei (1991) and Vecsei & Moussavian (1997); sample positions are indicated by gray arrows; Gran.= granule; Peb.= pebble; Cob.= cobble; Bou.= boulder.

pointing to a complex genesis resulting from the emersion, erosion, and downslope transport of the different kinds of shallow-water limestones occurring in the breccia (Fig. 9) (Moussavian & Vecsei 1995; Vecsei & Moussavian 1997). While some of these shallow-water limestones were clearly significantly reworked and altered during their transport from their original formation environment (i.e., the shallow portions of the platform) to their final depositional setting (i.e., the deeper portions of the platform), others moved downslope as coherent blocks (e.g., the LBF rudstones and the coral boundstones). They have sharp boundaries with the surrounding matrix and do not display evidence of mixing (e.g., presence of pelagic elements scattered within and thoroughly mixed with the shallow-water components). Transported material if not subject to extensive reworking and mixing with the surrounding slope sediments during transport can shed light on the environment where it was initially generated (Schlager 1991; Schlager et al. 1996; Coletti et al. 2015, 2016; Buček & Köhler 2017). Therefore, the Upper Cretaceous clasts and the Lower Paleocene clasts preserved in the Orfento and Santo Spirito formations can give us important information on the evolution of shallow-water, carbonate-producing assemblages of the Maiella platform across the K/Pg boundary and beyond.

Tab. 1 - Details of the skeletal assemblages of the LBF rudstone of VTG1, rudist-dominated floatstone to rudstone of VTG2, and coral boundstone of VTG3 and VTG4; counted samples are indicated, their position is indicated in Fig. 9; all the thin sections are stored at the Department of Earth and Environmental Sciences of the University of Milano-Bicocca.

	Upper Cretaceous		Lower Danian	
Section	**VTG1**	**VTG2**	**VTG3**	**VTG4**
Lithology	**LBF rudstone**	**Rudist floatstone to rudstone**	**Coral boundstone**	**Coral boundstone**
N° of counted sections	4	7	8	12
Samples	Roal1-4	E1-7	C1a-h	C3-7, R0, R1, R1bis-quater, R2, R2bis
Characteristics of the rock [point counting; %]				
Matrix	42	35	40	40
Prevailing type of matrix	Sparite; micrite	Comminuted bioclastic fragments (sand-sized)	Micrite	Micrite
Skeletal assemblage	58	65	60	60
Builders	22	57	55	56
Colonial corals	7.5	22	40	39
Composition of the skeletal assemblage [point counting; %]				
Colonial corals	13.0	34.5	66.0	65.0
Red calcareous algae	3.0	1.0	22.0	24.0
Green calcareous algae	0	0	1.5	1.5
LBF	53.5	9.0	0.0	0.0
SBF	2.5	1.5	1.5	2.0
Encrusting benthic foraminifera	4.0	6.0	4.5	5.0
Rudists	18.0	46.0	0.0	0.0
Other mollusks	0.5	0.0	1.0	0.5
Echinoderms	5.0	2.0	0.5	1.5
Bryozoans	0.5	0.0	2.5	0.5
Others	0.0	0.0	0.5	0

The Maiella platform in the aftermath of the end-Cretaceous extinction

Upper Cretaceous shallow-water carbonates are essentially dominated by either rudists or LBF (up to 45% and 53.5% of the skeletal assemblage respectively), associated with a significant contribution from colonial corals (13% in the LBF rudstone and 34.5% in the rudist floatstone to rudstone) (Tab. 1). In lower Danian assemblages, the first two groups are absent, whereas the latter has become significantly more abundant and dominates the skeletal assemblage (65-66%; Tab. 1). In the study area, similarly to other parts of the Adriatic and Apulian carbonate platforms (Drobne et al. 2007; Buček & Köhler 2017; Tešović et al. 2020), the K/Pg boundary is represented by a stratigraphic hiatus and the successions are not continuous (Fig. 9). However, this remarkable increase in the contribution of colonial corals to the skeletal assemblages is consistent with the findings of other authors: i.e., a relatively rapid recovery of hermatypic corals following the K/Pg mass extinction in comparison to other groups of carbonate producers such as LBF (Kiessling & Baron-Szabo 2004; Pandolfi & Kiessling 2014; Dishon et al. 2020; Tešović et al. 2020; Baron-Szabo et al. 2023; Martinuš et al. 2024).

In terms of the main groups of carbonate producers, lower Danian bioconstructions display a remarkable similarity with modern shallow-water coral reefs, as their framework is essentially built by corals and red calcareous algae (e.g., Hubbard et al. 1990; Harney & Fletcher 2003; Hart & Kench 2007; Perry et al. 2008). In the case of the investigated Danian bioconstructions the framework represents close to 60% of the total rock volume and is overwhelmingly dominated by colonial corals and red calcareous algae (which represent 65-66% and 22-24% of the entire skeletal assemblage, respectively) (Tab. 1). With regards to secondary carbonate producers, encrusting benthic foraminifera provide a minor contribution to the framework of both Danian and Upper Cretaceous bioconstructions (Tab. 1). While their ecological niche is still poorly understood, encrusting benthic foraminifera have been significantly contributing to shallow-water carbonates at least since the Late Jurassic (Granier 2024), with a peak during the Eocene (Plaziat & Perrin 1992; Coletti et al. 2022). The encrusting benthic foraminifera assemblage of the Danian bioconstructions of VTG is largely dominated by *Haddonia*-like agglutinated taxa. This is different from both younger Cenozoic bioconstructions and modern coral reefs, where encrusting hyaline and porcelaneous taxa prevail (e.g., Plaziat & Perrin 1992; Baceta et al. 2005; Tichenor & Lewis 2018; Coletti et al. 2021). Differently from modern reefs that develop in high-energy setting, the internal sediment of the Danian bioconstructions mainly consists of micrite (Tab. 1). This is not an isolated case. In many coral bioconstructions of the Paleocene micrite has been reported as the dominant type of internal sediment (Tab. 2) (Zamagni et al. 2008, 2009; Buček & Köhler 2017; Consorti & Köroğlu 2019; Vršič et al. 2021). There are also reports of coral bioconstructions associated with coarse-grained sediments (Accordi et al. 1998; Kiessling et al. 2005), but they are much less

Site	Central Italy VTG3	Central Italy VTG4	Pyrenean Basin Bz-2	Pyrenean Basin Lizarraga pass	Vel'ky Lipnik-Klippen Belt	Hazara Basin	Pyrenean Basin Leg-2	Hazara Basin
Age	Early Danian	Early Danian	Middle Danian	Late Danian	Selandian – early Thanetian	Selandian – early Thanetian	Thanetian	Late Thanetian
SBZ	SBZ1	SBZ1	SBZ1 - SBZ2	SBZ1 - SBZ2	SBZ3	SBZ3	SBZ3	SBZ3 to SBZ4
Reference	This work	This work	Baceta et al. 2005	Baceta et al. 2005	Köhler & Bucek 2005	Ali et al. 2024	Baceta et al. 2005	Ali et al. 2024
Characteristics of the rock								
Matrix	~ 1/3	~ 1/3	~ 1/2 - 3/4	~ 1/2 - 3/4	~ 1/3	~ 1/2	~ 4/5 - 2/3	~ 2/3
Skeletal assemblage	~ 2/3	~ 2/3	~ 1/4 - 1/2	~ 1/4 - 1/2	~ 2/3	~ 1/2	~ 1/5 - 1/3	~ 1/3
Type of matrix	Micrite	Micrite	Sand-sized bioclastic withn a peloidal micritic matrix	Sand-sized bioclastic	Micrite	Micrite	Micrite and microbioclasts	Micrite
Non skeletal grains	Rare - scarce	Scarce - common	Aggregated grains common at the reef crest; ooids in the back reef and in the lagoon	Aggregated grains common at the reef crest; ooids in the back reef and in the lagoon	Absent	Absent	Absent	Absent – very rare
Main frame builders	CC	CC	CC, RCA, calcareous sponges	CC, RCA, calcareous sponges	CC	CC	RCA , CC	CC
CC %	40	39	//	//	32	38	//	23.5
Secondary frame builders	RCA	RCA	EBF	EBF	RCA	//	EBF	RCA
Relative composition of the skeletal assemblage								
CC	Dominant (66.0)	Dominant (65.0)	Abundant	Abundant	Abundant (45)	Dominant (80.7)	Common	Dominant (62.2)
RCA	Common (22.0)	Common (24.0)	Abundant	Abundant	Abundant (28)	Absent	Common	Common (20.9)
GCA	Rare (1.5)	Rare (1.5)	Rare	Rare	Present	Rare (1.2)	Rare	Very-rare (0.5)
LBF	Absent	Absent	Absent	Absent	Present	Scarce (4.9)	Common	Scarce (5.4)
SBF	Rare (1.5)	Rare (2.0)	Common	Scarce	Present	Scarce (5.1)	Common	Rare (2.0)
EBF	Rare (4.5)	Scarce (5.0)	Scarce	Scarce	Common (12)	Absent	Scarce	Rare (2.5)
MOL	Very rare (1.0)	Very rare (0.5)	Rare	Scarce	Present	Scarce (5.1)	Scarce	Very-rare (0.7)
ECH	Very rare (0.5)	Rare (1.5)	Rare	Scarce	Present	Rare (2.0)	Rare	Rare (4.4)
BRY	Rare (2.5)	Very rare (0.5)	Scarce	Scarce	Present	Very-rare (0.8)	Common	Very-rare (0.9)
Others	Very rare (0.5)	Absent	Rare	Rare	Present	Very-rare (0.1)	Rare	Very-rare (0.4)
Foraminiferal assemblage	Entirely benthic	Entirely benthic	Entirely benthic	Entirely benthic	Mostly benthic	Entirely benthic	Entirely benthic	Entirely benthic
Dominant benthic taxa	Small hyaline, agglutinated and porcelaneous taxa	Small hyaline, agglutinated and porcelaneous taxa	Small and large hyaline taxa including miscellaneids	Small and large hyaline taxa including miscellaneids	Small and large hyaline taxa including miscellaneids, small and large porcelaneous taxa	Small hyaline taxa, small agglutinated taxa, miscellaneids	Large hyaline taxa including nummulitids, miscellaneids and orthophragmines and small hyaline taxa	Small hyaline taxa, miscellaneids

Tab. 2 - Comparison between the Paleocene coral bioconstructions of VTG, the bioconstruction from Vel'ky Lipnik of the Klippen Belt of Slovakia (Köhler & Bucek 2005), those from the Ghumanwan Section of the Hazara Basin (Ali et al. 2024), and those from the Pyrenees (Baceta et al. 2005). The relative abundance of the various components is given using a modified version of the scale proposed by Carey et al. (1995): 0% = absent; 1% > very rare > 0%; 5% > rare > 1%; 10% > scarce > 5%; 25% > common > 10%; 50% > abundant > 25%; dominant > 50%. CC= colonial corals; RCA= red calcareous algae; GCA= green calcareous algae; LBF= larger benthic foraminifera; SBF= small benthic foraminifera; EBF= encrusting benthic foraminifera; MOL= mollusks; ECH= echinoderms; BRY= bryozoans.

common. This suggests that most of the known coral-dominated bioconstructions of the Paleocene, including those investigated in the current research, likely developed in a more calm and protected (and thus possibly deeper) environment than most of their modern counterparts. With regards to water depth, the overall skeletal assemblage suggests a placement within the photic zone. Given the lack of planktic foraminifera, the low abundance of porcelaneous foraminifera, and the presence of both green and red calcareous algae, it is possible to exclude that the investigated bioconstructions developed in extremely shallow settings or close to the lower limit of the photic zone. Unfortunately, both green algae and foraminifera are too rare (1.5% and 1.5-2% of the skeletal assemblage, respectively) to provide more useful information. Red calcareous algae are far more abundant but the assemblage, is dominated by Sporolithales and Peyssonneliales, whereas Hapalidiales and Corallinales are rare. The depth distributions of the latter two groups are well known in modern oceans and have been used to create reliable paleobathymetric reconstructions (Coletti & Basso 2020). The scarcity of Hapalidiales and Corallinales prevents more detailed reconstruction based on red calcareous algae. The transported nature and the poor exposure of the investigated boundstones also prevent paleobathymetric interpretations based on the overall geometry of the outcrop. Consequently, while it is clear that these bioconstructions formed within the photic zone in a low-energy environment, the data currently available cannot provide a definitive answer on whether they originated in the upper, middle, or lower part of the photic zone.

The Late Paleocene crisis of coral carbonate production

Comparing VTG coral bioconstructions to other Paleocene coral-dominated structures reveals a general decline in the overall contribution of corals to carbonate production during the Paleocene (Tab. 2: CC %). This decline is particularly relevant during the late Thanetian (Tab. 2) (Baceta

et al. 2005). A similar pattern can be seen in the abundance of shallow-water coral-dominated facies. The latter, from the late Thanetian until the end of the Middle Eocene, are quite rare (Kiessling & Simpson 2011; Zamagni et al. 2012; Coletti et al. 2022). Corals still occur during the whole Early to Middle Eocene interval and they display reef-building capacity (e.g., Baceta et al. 2005; Vescogni et al. 2016; Martin-Martin et al. 2023; Benedetti et al. 2024), but they are much less common than other groups of shallow-water carbonate producers, such as LBF (Pomar et al. 2017; Coletti et al. 2022). The results of the quantitative analysis of the Danian skeletal assemblages from Maiella further support this overall pattern resulting from the analysis of the abundance of coral bioconstructions, highlighting a late Thanetian crisis in coral carbonate production in shallow-waters. This crisis seems to have only affected coral's ability to accumulate large quantities of calcium carbonate, not their biodiversity (Bosellini et al. 2022; Benedetti et al. 2024), and it has been linked to various environmental factors, including nutrient availability, ocean chemistry and circulation, biological evolution and, last but not least, temperature (e.g., Baceta et al. 2005; Scheibner & Speijer 2008; Zamagni et al. 2009, 2012; Pomar et al. 2017; Coletti et al. 2022; Ali et al. 2024). The Paleocene was characterized by a general warming trend starting from ca. 61-58 Ma (Selandian – earliest Thanetian), culminating during the latest Thanetian – earliest Eocene, and followed by a prolonged period of elevated temperatures spanning most of the Early and Middle Eocene (Zachos et al. 2001; Barnet et al. 2019). Afterwards global temperatures gradually dropped and continued to do so until the Late Oligocene Warming (Zachos et al. 2001). Within the Tethys, during the same time interval, colonial corals carbonate production seems to be negatively correlated with temperature, decreasing from the Danian to the late Thanetian, reaching a minimum during the Early and Middle Eocene and increasing during the Late Eocene and the Oligocene (Coletti et al. 2022). Coral biodiversity does not reflect this and appears to be somewhat unrelated to the overall rate of calcium carbonate production and accumulation (Benedetti et al. 2024), in agreement with the conclusion of Jonson et al. (2008) for the Caribbean. Despite these seeming contradictions and the scarcity of quantitative data, it is possible to propose an overall explanation that combines the evidence based on the composition of skeletal assemblages (this work), with the distribution and frequency of coral dominated facies (Kiessling et al. 1999; Zamagni et al. 2012; Coletti et al. 2022), and data on coral biodiversity (Benedetti et al. 2024). Large, coral-dominated bioconstructions appear less likely to develop during warm periods, particularly during those marked by a rapid and remarkable rise in temperature over a geologically short time span, such as during the late Thanetian (Kiessling et al. 1999; Zamagni et al. 2012; Coletti et al. 2022). While large bioconstructions during these time intervals might be rare, colonial corals are usually able to survive, and (possibly pushed to diversification by the adverse conditions) to even gain biodiversity, especially if temperatures are rising gradually (Vescogni et al. 2016; Bendetti et al. 2024). This in turn may open new niches for corals and possibly allows them to better colonize "refuge areas" like the mesophotic zone, where they can more easily endure warm periods (e.g., Morsilli et al. 2012; Pomar & Hallock 2007; Pomar et al. 2017). This wider perspective suggests that colonial corals, as a group, are indeed resilient to a wide variety of adverse events, including climate change. However, reefs (considered as complex, bioconstructed, shallow-water ecosystems where corals play a major role) are severely affected by processes like global warming and may take a geologically long time to recover.

Conclusions

The limestones of the Maiella massif hold a wealth of information about the evolution and distribution of shallow-water carbonate producers over critical time intervals such as the Late Cretaceous and Early Paleogene. The current research indicates that colonial corals were a significant part of the skeletal assemblage of the Upper Cretaceous shallow-water carbonates and that their abundance notably increased in the Lower Paleocene. This suggests a faster recovery of corals from the Cretaceous–Paleogene extinction compared to other groups of neritic carbonate producers such as larger benthic foraminifera. The comparison between the Lower Paleocene coral bioconstructions of the Maiella massif and others formed later during the remainder of the Paleocene reveals an overall de-

cline in coral carbonate production with a minimum in the uppermost Paleocene. Quantitative microfacies analysis clearly allows for the recognition of this trend, enabling the refinement of data on carbonate production resulting from the study of the frequency of coral-dominated facies. The latter studies show that, at least in the Tethys, coral carbonate production did not recover until the Late Eocene. This overall pattern appears to be linked to average global temperatures, which progressively increased during the Late Paleocene, peaked during the latest Paleocene - Early Eocene interval, remained elevated for most of the Middle Eocene, and decreased thereafter. Water chemistry, biological evolution, nutrient availability, and ocean circulation most likely also had an impact.

The current analysis based on the composition of skeletal assemblages provides evidence for both the recovery of shallow-water corals carbonate production after the end-Cretaceous extinction and its Late Paleocene decline. This supports the existing data on coral-dominated facies and integrates with the data on coral biodiversity, providing an overall picture of coral carbonate production during the Cenozoic. Warm periods, especially those characterized by rapidly rising temperatures, seem to be unfavorable for the development of large, coral-dominated, bioconstructions. Colonial corals continue to exist during these times, and their biodiversity may even rise, allowing them to better spread in ecological niches more shielded from the high temperatures (e.g., the mesophotic zone). This indicates that colonial corals are able to endure severe crises by adapting to the changing environmental conditions. However, coral bioconstructions are susceptible to warming events (especially rapid ones) and, although corals as a group can survive these events, their contribution to shallow-water reefs may significantly decline.

Acknowledgements. The authors are grateful to the Parco Nazionale della Maiella and in particular to Professor Lucio Zazzara for authorizing our research. The authors, and in particular G.C., would also like to express their gratitude towards Prof. Francesco Sabatini, his never-ending activism towards his homeland, his passion for scientific research, his curiosity and his kindness have all been invaluable elements in developing this research project. Special thanks also to Prof. Eduardo Garzanti and Dr. Or M. Bialik for the precious insights and the fruitful discussions, to the reviewers that provided useful insights to improve this paper, and to the editors for the patience and their support. This article represents an outcome of the Projec TECLA - Dipartimenti di Eccellenza 2023_2027, funded by MIUR and a contribution to Research project PID2022-137860NB-I00 funded by the MCIN/ AEI / 10.13039/501100011033 / FEDER, UE).

References

Accarie H. (1988) - Dynamique sédimentaire et structurale au passage plateforme/bassin. Les faciès carbonatés crétacés et tertiaires: Massif de la Maiella (Abruzzes, Italie). *École des Mines de Paris, Mémoires Science de la Terre*, 5.

Accordi G., Carbone F. & Pignatti J. (1998) - Depositional history of a Paleogene carbonate ramp (western Cephalonia, Ionian Islands, Greece). *Geologica Romana*, 34: 131-205.

Aguilera O., Bencomo K., Araújo O.M.O. de, Dias B.B., Coletti G., Lima D., Silane A.F., Polk M., Alves-Martin M.V., Jaramillo C., Kutter V.T. & Lopes R.T. (2020) - Miocene heterozoan carbonate systems from the western Atlantic equatorial margin in South America: The Pirabas Formation. *Sedimentary Geology*, 407: 1-28. https://doi.org/10.1016/j.sedgeo.2020.105739.

Ali M., Coletti G., Mariani L., Benedetti A., Munawar M.J., Rehman S.U., Sternai P., Basso D., Malinverno E., Shahzad K., Khan S., Awais M., Usman M., Castelltort S., Adatte T. & Garzanti E. (2024) - Shallow-water carbonate facies herald the onset of the Palaeocene-Eocene Thermal Maximum (Hazara basin, Northern Pakistan). *Journal of Asian Earth Sciences: X*, 11: 100169.

Aubry M.P., Piller W.E., Van Couvering J.A., Berggren W.A., Flynn J.J., Head M.J., Hilgen F., Tian J., Kent D.V. & Miller K.G. (2023) - Unifying Cenozoic chronostratigraphy and geochronology: applying the rules. *Newsletters on Stratigraphy*, 57: 25-36. DOI: 10.1127/nos/2023/0767.

Baceta J.I., Victoriano P. & Bernaola G. (2005) - Paleocene coralgal reefs of the western Pyrenean basin, northern Spain: New evidence supporting an earliest Paleogene recovery of reefal ecosystems. *Palaeogeography, Palaeoclimatology, Palaeoecology*, 224(1-3): 117-143.

Barattolo F. (1998) - Dasycladacean green algae and microproblematica of the uppermost Cretaceous–Paleocene in the Karst area (NE Italy and Slovenia). In: Hottinger L. & Drobne K. (Eds.) - Paleogene shallow benthos of the Tethys: 65-127. Opera Dela Slovenske akademije znanosti in umetnosti (SAZU), Ljubljana.

Barnet J. S., Littler K., Westerhold T., Kroon D., Leng M. J., Bailey I., Rohl U. & Zachos J.C. (2019) - A high-fidelity benthic stable isotope record of late Cretaceous–early Eocene climate change and carbon-cycling. *Paleoceanography and Paleoclimatology*, 34(4): 672-691.

Baron-Szabo R. C., Schlagintweit F. & Rashidi K. (2023) - Coral fauna across the Cretaceous–Paleogene boundary at Zagros and Sistan Suture zones and Yazd Block of Iran. *Swiss Journal of Palaeontology*, 142(1): 1-49.

Benedetti A. (2019) - Benthic foraminiferal assemblages from the late Eocene to the early Oligocene of the Caltavuturo Formation in the Madonie Mountains (Sicily): a tool for correlation. *Italian Journal of Geosciences*, 138(1): 43-55.

Benedetti A. & Papazzoni C.A. (2022) - Rise and fall of rotaliid foraminifera across the Paleocene and Eocene times. *Micropaleontology*, 68(2): 185-196.

Benedetti A., Papazzoni C.A. & Bosellini F.R. (2024) - Unparallel resilience of shallow-water tropical calcifiers (foraminifera and scleractinian reef corals) during the early Paleogene global warming intervals. *Palaeogeography, Palaeoclimatology, Palaeoecology*, 651: 112393.

Bellwood D.R., Hoey A.S., Ackerman J.L. & Depczynski M. (2006) - Coral bleaching, reef fish community phase

shifts and the resilience of coral reefs. *Global Change Biology*, 12(9): 1587-1594.

Bernoulli D., Anselmetti F., Eberli G., Mutti M., Pignatti J., Sanders D. & Vecsei A. (1996) - Montagna della Maiella: the sedimentary and sequential evolution of a Bahamian-type carbonate platform of the South-Tethyan continental margin. *Memorie della Società Geologica Italiana*, 51: 7-12.

Bialik O.M., Coletti G., Mariani L., Commissario L., Desbiolles F. & Meroni A.N. (2023) - Availability and type of energy regulate the global distribution of neritic carbonates. *Scientific Reports*, 13(1): 19687.

Birkeland C. (1997) - Life and death of coral reefs. Springer Science & Business Media, New York, NY, USA, 536 pp.

Bosellini F. & Russo A. (1995) - The Scleractinian genus *Actinacis*. Systematic revision and stratigraphic record of the Tertiary species with special regard to Italian occurrences. *Rivista italiana di Paleontologia e Stratigrafia*, 101: 215-230.

Bosellini F.R. & Perrin C. (2008) - Estimating Mediterranean Oligocene–Miocene sea-surface temperatures: an approach based on coral taxonomic richness. *Palaeogeography, Palaeoclimatology, Palaeoecology*, 258(1-2): 71-88.

Bosellini F.R., Vescogni A., Budd A.F. & Papazzoni C.A. (2021) - High coral diversity is coupled with reef-building capacity during the Late Oligocene Warming Event (Castro Limestone, Salento Peninsula, S Italy). *Rivista Italiana di Paleontologia e Stratigrafia*, 127(3): 515-538.

Bosellini F.R., Benedetti A., Budd A.F. & Papazzoni C.A. (2022) - A coral hotspot from a hot past: The EECO and post-EECO rich reef coral fauna from Friuli (Eocene, NE Italy). *Palaeogeography, Palaeoclimatology, Palaeoecology*, 607: 111284.

Brandano M., Lipparini L., Campagnoni V. & Tomassetti L. (2012) - Downslope-migrating large dunes in the Chattian carbonate ramp of the Majella Mountains (Central Apennines, Italy). *Sedimentary Geology*, 255: 29-41.

Brandano M., Cornacchia I., Raffi I. & Tomassetti L. (2016a) - The Oligocene–Miocene stratigraphic evolution of the Majella carbonate platform (Central Apennines, Italy). *Sedimentary Geology*, 333: 1-14.

Brandano M., Tomassetti L., Sardella R. & Tinelli C. (2016b) - Progressive deterioration of trophic conditions in a carbonate ramp environment: the *Lithothamnion* Limestone, Majella Mountain (Tortonian–early Messinian, central Apennines, Italy). *Palaios*, 31(4): 125-140.

Brandano M., Tomassetti L., Cornacchia I., Trippetta F., Pomar L. & Petracchini L. (2020) - The submarine dune field of the Bolognano Fm. Depositional processes and the carbonate reservoir potential (Chattian to Burdigalian, Majella Carbonate Platform). *Geological Field Trips & Maps*, 12(2.3): 1-42.

Brandano M., Tomassetti L., Di Bella L., Barberio D.M., Barbieri M. & Ferrini A. (2022) - Late Burdigalian to early Messinian environmental and climatic evolution of the central paleo Adriatic domain from the shallow water sedimentary record (Bolognano Fm, Eastern Majella, Central Apennines). *Sedimentary Geology*, 440: 106235.

Bryant D., Burke L., McManus J. & Spalding M. (1998) - Reefs at risk: a map-based indicator of threats to the world's coral reefs. World Resources Institute, New York, USA, 57 pp.

Buček S. & Köhler E. (2017) - Palaeocene Reef Complex of the Western Carpathians. *Slovak Geological Magazine*, 17(1): 3-163.

Carey J.S., Moslow T.F. & Barrie J.V. (1995) - Origin and distribution of Holocene temperate carbonates, Hecate Strait, western Canada continental shelf. *Journal of Sedimentary Research*, 65(1a): 185-194.

Cheung M.W., Hock K., Skirving W. & Mumby P.J. (2021) - Cumulative bleaching undermines systemic resilience of the Great Barrier Reef. *Current biology*, 31(23): 5385-5392.

Chiocchini M. & Mancinelli A. (2001) - *Sivasella monolateralis* Sirel and Gunduz, 1978 (Foraminiferida) in the Maastrichtian of Latium (Italy). *Revue de Micropaléontologie*, 44(4): 267-277.

Cipriani M., Apollaro C., Basso D., Bazzicalupo P., Bertolino M., Bracchi V.A., Bruno F., Costa G., Dominici R., Gallo A., Muzzupappa M., Rosso A., Sanfilippo R., Sciuto F., Vespasiano G. & Guido A. (2024) - Origin and role of non-skeletal carbonate in coralligenous build-ups: new geobiological perspectives in biomineralization processes. *Biogeosciences*, 21: 49-72.

Coletti G., Basso D., Frixa A. & Corselli C. (2015) - Transported rhodoliths witness the lost carbonate factory: a case history from the Miocene Pietra da Cantoni limestone (NW Italy). *Rivista Italiana di Paleontologia e Stratigrafia*, 121(3): 345-368.

Coletti G., Vezzoli G., Di Capua A. & Basso D. (2016) - Reconstruction of a lost carbonate factory based on its biogenic detritus (Ternate-Travedona Formation and Gonfolite Lombarda Group-Northern Italy). *Rivista Italiana di Paleontologia e Stratigrafia*, 122: 1-22.

Coletti G. & Basso D. (2020) - Coralline algae as depth indicators in the Miocene carbonates of the Eratosthenes Seamount (ODP Leg 160, Hole 966F). *Geobios*, 60: 29-46.

Coletti G., Balmer E.M., Bialik O.M., Cannings T., Kroon D., Robertson A.H. & Basso D. (2021) - Microfacies evidence for the evolution of Miocene coral-reef environments in Cyprus. *Palaeogeography, Palaeoclimatology, Palaeoecology*, 584: 110670.

Coletti G., Commissario L., Mariani L., Bosio G., Desbiolles F., Soldi M. & Bialik O. M. (2022) - Palaeocene to Miocene southern Tethyan carbonate factories: A meta-analysis of the successions of South-western and Western Central Asia. *The Depositional Record*, 8(3): 1031-1054.

Consorti L. & Köroğlu F. (2019) - Maastrichtian-Paleocene larger Foraminifera biostratigraphy and facies of the Şahinkaya Member (NE Sakarya Zone, Turkey): Insights into the Eastern Pontides arc sedimentary cover. *Journal of Asian Earth Sciences*, 183: 103965.

Consorti L. & Schlagintweit F. (2022) - Taxonomy and paleoecology of the Maastrichtian-Paleogene benthic foraminifer Valvulineria orali (Inan, 2003) comb. nov. *Journal of Mediterranean Earth Sciences*, 14: 1-9.

Cornacchia I., Andersson P., Agostini S., Brandano M. & Di Bella L. (2017) - Strontium stratigraphy of the upper Miocene *Lithothamnion* Limestone in the Majella Mountain, central Italy, and its palaeoenvironmental implications. *Lethaia*, 50(4): 561-575.

Cornacchia I., Brandano M., Raffi I., Tomassetti L. & Flores I. (2018) - The Eocene–Oligocene transition in the C-isotope record of the carbonate successions in the Central Mediterranean. *Global and Planetary Change*, 167: 110-122.

Cornacchia I., Brandano M. & Agostini S. (2021) - Miocene paleoceanographic evolution of the Mediterranean area and carbonate production changes: A review. *Earth-Sci-*

ence Reviews, 221: 103785.

Crescenti U., Crostella A., Donzelli G. & Raffi G. (1969) - Stratigrafia della serie calcarea dal Lias al Miocene nella regione marchigiano-abruzzese (Parte II. Litostratigrafia, Biostratigrafia, Paleogeografia). *Memorie Società Geologica Italiana*, 8(2): 343-420.

Descombes P., Wisz M.S., Leprieur F., Parravicini V., Heine C., Olsen S.M., Swingedouw D., Kulbiki M., Moutillout D. & Pellissier L. (2015) - Forecasted coral reef decline in marine biodiversity hotspots under climate change. *Global Change Biology*, 21(7): 2479-2487.

Dishon G., Grossowicz M., Krom M., Guy G., Gruber D.F. & Tchernov D. (2020) - Evolutionary traits that enable scleractinian corals to survive mass extinction events. *Scientific Reports*, 10: 3903.

Drobne K., Ogorelec B. & Riccamboni R. (2007) - *Bangiana hanseni* n. gen. n. sp. Foraminifera, and index species of Danian age (Lower Paleocene) from the Adriatic Carbonate Platform (SW Slovenia, NE Italy, Herzegovina). *Razprave 4.Razreda, Slovenska Akademija Znanosti in Umetnosti (SAZU)*, 45: 5-71.

Eberli G.P., Bernoulli D., Sanders D. & Vecsei A. (1993) - From Aggradation to Progradation: The Maiella Platform, Abruzzi, Italy. In: Simo T., Scott R.W., Masse J.P. (Eds.), Cretaceous Carbonate Platforms. *American Association of Petroleoum Geologist Memories*, 56: 213-232.

Eberli G.P., Bernoulli D., Vecsei A., Sekti R., Grasmueck M., Lüdmann T., Anselmetti F.S., Mutti M. & Della Porta G. (2019) - A Cretaceous carbonate delta drift in the Montagna della Maiella, Italy. *Sedimentology*, 66(4): 1266-1301.

Flügel E. & Flügel-Kahler E. (1992) - Phanerozoic reef evolution: basic questions and data base. *Facies*, 26: 167-277.

Flügel E. (2010) - Microfacies of Carbonate Rocks: Analysis Interpretation and Application. Springer, New York, 984 pp.

Granier B.R. (2024) - Reassessment of *Iberopora bodeuri*, a primitive plurilocular calcareous encrusting foraminifer from the "Upper Jurassic" (including Berriasian) carbonate platforms of the northern and central Tethys. *Cretaceous Research*, 155: 105782.

Harney J.N. & Fletcher III C.H. (2003) - A budget of carbonate framework and sediment production, Kailua Bay, Oahu, Hawaii. *Journal of Sedimentary Research*, 73(6): 856-868.

Hart D.E. & Kench P.S. (2007) - Carbonate production of an emergent reef platform, Warraber Island, Torres Strait, Australia. *Coral Reefs*, 26: 53-68.

Hubbard D.K., Miller A.I. & Scaturo D. (1990) - Production and cycling of calcium carbonate in a shelf-edge reef system (St. Croix, US Virgin Islands); applications to the nature of reef systems in the fossil record. *Journal of Sedimentary Research*, 60(3): 335-360.

Inan N., Tasli K. & Inan S. (2005) - *Laffitteina* from the Maastrichtian-Paleocene shallow marine carbonate successions of the Eastern Pontides (NE Turkey): biozonation and microfacies. *Journal of Asian Earth Sciences*, 25(2): 367-378.

Johnson K.G., Jackson J.B. & Budd A.F. (2008) - Caribbean reef development was independent of coral diversity over 28 million years. *Science*, 319(5869): 1521-1523.

Kato A., Baba M., Kawai H. & Masuda M. (2006) - Reassessment of the little-known crustose red algal genus Polystrata (Gigartinales), based on morphology and SSU rDNA sequences. *Journal of Phycology*, 42(4): 922-933.

Kiessling W., Flügel E. & Golonka J. (1999) - Paleoreef maps: evaluation of a comprehensive database on Phanerozoic reefs. *American Association of Petroleoum Geologist Bulletin*, 83(10): 1552-1587.

Kiessling W., Flügel E. & Golonka J. (2003) - Patterns of Phanerozoic carbonate platform sedimentation. *Lethaia*, 36(3): 195-225.

Kiessling W. & Baron-Szabo R.C. (2004) - Extinction and recovery patterns of scleractinian corals at the Cretaceous-Tertiary boundary. *Palaeogeography, Palaeoclimatology, Palaeoecology*, 214(3): 195-223.

Kiessling W., Aragón E., Scasso R., Aberhan M., Kriwet J., Medina F. & Fracchia D. (2005) - Massive corals in Paleocene siliciclastic sediments of Chubut (Argentina). *Facies*, 51: 233-241.

Kiessling W. & Simpson C. (2011) - On the potential for ocean acidification to be a general cause of ancient reef crises. *Global Change Biology*, 17(1): 56-67.

Kiessling W. & Kocsis Á. T. (2015) - Biodiversity dynamics and environmental occupancy of fossil azooxanthellate and zooxanthellate scleractinian corals. *Paleobiology*, 41(3): 402-414.

Knowlton N., Brainard R.E., Fischer R., Moews M., Plaisance L. & Caley M.J. (2010) - Coral reef biodiversity. In: McIntyre A.D. (Ed.) - Life in the World's Oceans: Diversity Distribution: 65-74. Wiley-Blackwell, Oxford, UK.

Köhler E. & Bucek S. (2005) - Paleocene reef limestones near Velký Lipnık (Pieniny Mts, NE Slovakia): facial environment and biogenic components. *Slovak Geological Magazine*, 11: 249-267.

Lampert S.A., Lowrie W., Hirt A.M., Bernoulli D. & Mutti M. (1997) - Magnetic and sequence stratigraphy of redeposited Upper Cretaceous limestones in the Montagna della Maiella, Abruzzi, Italy. *Earth and Planetary Science Letters,* 150(1-2): 79-93.

Martín-Martín M., Tosquella J., Guerrera F., Maaté A., Hlila R., Maaté S., Tramontana M. & Le Breton E. (2023) - The Eocene carbonate platforms of the Ghomaride Domain (Internal Rif Zone, N Morocco): A segment of the westernmost Tethys. *Sedimentary Geology*, 106423.

Martinuš M., Tešović B. C., Jurić S. & Vlahović I. (2024) - Patch reefs with scleractinian corals and layered domical and bulbous growth forms (calcified sponges?) in the upper Maastrichtian and lowermost Palaeocene platform carbonates, Adriatic islands of Brač and Hvar (Croatia). *Palaeogeography, Palaeoclimatology, Palaeoecology*, 112056.

Moberg F. & Folke C. (1999) - Ecological goods and services of coral reef ecosystems. *Ecological economics*, 29(2): 215-233.

Morsilli M., Rusciadelli G. & Bosellini A. (2002) - Large-scale gravity-driven structures: control on margin architecture and related deposits of a Cretaceous Carbonate Platform (Montagna della Maiella, Central Apennines, Italy). *Bollettino Società Geolica Italiana*, Special Vol. 1: 619-628.

Morsilli M., Bosellini F.R., Pomar L., Hallock P., Aurell M. & Papazzoni C.A. (2012) - Mesophotic coral buildups in a prodelta setting (late Eocene, southern Pyrenees, Spain): a mixed carbonate–siliciclastic system. *Sedimentology*, 59(3): 766-794.

Moussavian E. & Vecsei A. (1995) - Paleocene reef sediments from the Maiella carbonate platform, Italy. *Facies*, 32(1): 213-221.

Muttoni G., Dallanave E. & Channell J.E.T. (2013) - The drift history of Adria and Africa from 280 Ma to Present,

Jurassic true polar wander, and zonal climate control on Tethyan sedimentary facies. *Palaeogeography, Palaeoclimatology, Palaeoecology*, 386: 415-435.

Nicolai C. & Gambini R. (2007) - Structural architecture of the Adria platform-and-basin system. *Bollettino della Società Geologica Italiana*, 7: 21-37.

Özcan E., Yücel A.O., Catanzariti R., Kayğılı S., Okay A.I., Simmons M.D., Pignatti J., Abbasi İ.A. & Erbil Ü. (2021) - Multiple *Orbitoides* d'Orbigny lineages in the Maastrichtian? Data from the Central Sakarya Basin (Turkey) and Arabian Platform successions (Southeastern Turkey and Oman). *Swiss Journal of Palaeontology*, 140: 1-30.

Pandolfi J.M. & Kiessling W. (2014) - Gaining insights from past reefs to inform understanding of coral reef response to global climate change. *Current Opinion in Environmental Sustainability*, 7: 52-58.

Papazzoni C.A., Fornaciari B., Giusberti L., Simonato M. & Fornaciari E. (2023) - A new definition of the Paleocene Shallow Benthic Zones (SBP) by means of larger foraminiferal biohorizons, and their calibration with calcareous nannofossil biostratigrapy. *Micropaleontology*, 69(4): 363-399.

Paulay G. (1997) - Diversity and distribution of reef organisms. In: Birkeland C. (Ed.) - Life and death of coral reefs: 298-353. Chapman Hall, London.

Pestana E.M.D.S., Nunes J.M.D.C., Cassano V. & Lyra G.D.M. (2021) - Taxonomic revision of the Peyssonneliales (Rhodophyta): Circumscribing the authentic *Peyssonnelia* clade and proposing four new genera and seven new species. *Journal of Phycology*, 57(6): 1749-1767.

Perrin C. (1992) - Signification écologique des foraminifères acervulinidés et leur rôle dans la formation de faciès récifaux et organogènes depuis le Paléocène. *Geobios*, 25(6): 725-751.

Perry C.T., Spencer T. & Kench P.S. (2008) - Carbonate budgets and reef production states: a geomorphic perspective on the ecological phase-shift concept. *Coral Reefs*, 27: 853-866.

Plaziat J.C. & Perrin C. (1992) - Multikilometer-sized reefs built by foraminifera (*Solenomeris*) from the early Eocene of the Pyrenean domain (S. France, N. Spain): Palaeoecologic relations with coral reefs. *Palaeogeography, Palaeoclimatology, Palaeoecology*, 96(3-4): 195-231.

Pomar L., Brandano M. & Westphal H. (2004) - Environmental factors influencing skeletal grain sediment associations: a critical review of Miocene examples from the western Mediterranean. *Sedimentology*, 51(3): 627-651.

Pomar L. & Hallock P. (2007) - Changes in coral-reef structure through the Miocene in the Mediterranean province: Adaptive versus environmental influence. *Geology*, 35: 899-902.

Pomar L. & Hallock P. (2008) - Carbonate factories: a conundrum in sedimentary geology. *Earth-Science Reviews*, 87(3-4): 134-169.

Pomar L., Bassant P., Brandano M., Ruchonnet C. & Janson X. (2012) - Impact of carbonate producing biota on platform architecture: insights from Miocene examples of the Mediterranean region. *Earth-Science Reviews*, 113: 186-211.

Pomar L., Baceta J.I., Hallock P., Mateu-Vicens G. & Basso D. (2017) - Reef building and carbonate production modes in the west-central Tethys during the Cenozoic. *Marine and Petroleum Geology*, 83: 261-304.

Raffi I., Ricci C., Garzarella A., Brandano M., Cornacchia I. & Tomassetti L. (2016) - Calcareous nannofossils as a dating tool in shallow marine environment: an example from an upper Paleogene carbonate platform succession in the Mediterranean. *Newsletters on Stratigraphy*, 49(3): 481-495.

Robles-Salcedo R., Vicedo V. & Caus E. (2018) - Latest Campanian and Maastrichtian Siderolitidae (larger benthic foraminifera) from the Pyrenees (S France and NE Spain). *Cretaceous Research*, 81: 64-85.

Rusciadelli G. (2005) - The Maiella Escarpment (Apulia platform, Italy): geology and modelling of an Upper Cretaceous scalloped erosional platform margin. *Bollettino della Società geologica Italiana*, 124: 661-673.

Rusciadelli G., Sciarra N. & Mangifesta M. (2003) - 2D modelling of large-scale platform margin collapses along an ancient carbonate platform edge (Maiella Mt., Central Apennines, Italy): geological model and conceptual framework. *Palaeogeography, Palaeoclimatology, Palaeoecology*, 200(1-4): 245-262.

Rusciadelli G. & Di Simone S. (2007) - Differential compaction as a control on depositional architectures across the Maiella carbonate platform margin (central Apennines, Italy). *Sedimentary Geology*, 196(1-4): 133-155.

Sani F., Vannucci G., Boccaletti M., Bonini M., Corti G. & Serpelloni E. (2016) - Insights into the fragmentation of the Adria Plate. *Journal of Geodynamics*, 102: 121-138.

Sartorio D. & Venturini S. (1988) - Southern Tethys Biofacies. Agip, Amilcare Pizzi, Italy, pp. 236.

Scheibner C. & Speijer R.P. (2008) - Late Paleocene–early Eocene Tethyan carbonate platform evolution - A response to long-and short-term paleoclimatic change. *Earth-Science Reviews*, 90(3-4): 71-102.

Schlager W. (1991) - Depositional bias and environmental change—important factors in sequence stratigraphy. *Sedimentary Geology*, 70(2-4): 109-130.

Schlager W., Reijmer J.J. & Droxler A. (1994) - Highstand shedding of carbonate platforms. *Journal of Sedimentary Research*, 64(3b): 270-281.

Schmitz B., Pujalte V., Molina E., Monechi S., Orue-Etxebarria X., Speijer R.P., Alegret L., Apellaniz E., Arenillas I., Aubry M.P., Baceta J.I., Berggren W.A., Bernaola G., Caballero F., Clemmensen A., Dinarès-Turell J., Dupuis C., Heilmann-Clausen C., Orús A.H., Knox R., Martín-Rubio M., Ortiz S., Payros A., Petrizzo M.R., Salis K. von, Sprong J., Steurbaut E. & Thomsen E. (2011) - The global stratotype sections and points for the bases of the Selandian (Middle Paleocene) and Thanetian (Upper Paleocene) stages at Zumaia, Spain. *Episodes*, 34: 220-243

Serra-Kiel J., Hottinger L., Caus E., Drobne K., Ferrandez C., Jauhri A.K., Less G., Pavlovec R., Pignatti J., Samso J.M., Schaub H., Sirel E., Strougo A., Tambareau Y., Tosquella J. & Zakrevskaya E. (1998) - Larger foraminiferal biostratigraphy of the Tethyan Paleocene and Eocene. *Bulletin de la Société Géologique de France*, 169: 281-299.

Serra-Kiel J., Vicedo V., Baceta J.I., Bernaola G. & Robador A. (2020) - Paleocene larger foraminifera from the Pyrenean Basin with a recalibration of the Paleocene shallow benthic zones. *Geologica Acta*, 18: 1-III.

Sinanoğlu D., Benedetti A. & Özgen-Erdem N. (2022) - Danian (SBZ2) larger foraminifera from the Becirman Formation (southeastern Turkey) as evidence of rotalids diversity in lower Paleocene shallow-water environments. *Rivista Italiana di Paleontologia e Stratigrafia,* 128(2): 431-452.

Stolarski J., Bosellini F.R., Wallace C.C., Gothmann A.M., Mazur M., Domart-Coulon I., Gutner-Hoch E., Neuser R.D., Levy O., Shemesh A. & Meibom A. (2016) - A unique coral biomineralization pattern has resisted 40 million years of major ocean chemistry change. *Scientific Reports*, 6(1): 27579.

Tešović B.C., Martinuš M., Golec I. & Vlahović I. (2020) - Lithostratigraphy and biostratigraphy of the uppermost Cretaceous to lowermost Palaeogene shallow-marine succession: top of the Adriatic Carbonate Platform at the Likva Cove section (island of Brač, Croatia). *Cretaceous Research*, 114: 104507.

Tichenor H.R. & Lewis R.D. (2018) - Distribution of encrusting foraminifera at San Salvador, Bahamas: a comparison by reef types and onshore−offshore zonation. *Journal of Foraminiferal Research*, 48(4): 373-387.

Vecsei A. (1991) - Aggradation und Progradation eines Karbonatplattform-Randes: Kreide bis mittleres Tertiar der Montagna della Maiella, Abruzzen. - *Mitteilungen aus dem Geologischen Institut der Eidgenössischen Technischen Hochschule und der Universität Zürich, Neue Folge*, 294: 1-169.

Vecsei A. & Moussavian E. (1997) - Paleocene reefs on the Maiella platform margin, Italy: an example of the effects of the Cretaceous/Tertiary boundary events on reefs and carbonate platforms. *Facies*, 36: 123-139.

Vecsei A., Sanders D.G., Bernoulli D., Eberli G.P. & Pignatti J.S. (1998) - Cretaceous to Miocene sequence stratigraphy and evolution of the Maiella carbonate platform margin, Italy. In: Graciansky P.C. de, Hardenbol J., Jacquin T. & Vail P.R. (Eds.) - Mesozoic and Cenozoic Sequence Stratigraphy of European Basins: 53-74. SEPM Society for Sedimentary Geology, Special Publication, 60.

Vecsei A. & Sanders D.G. (1999) - Facies analysis and sequence stratigraphy of a Miocene warm-temperate carbonate ramp, Montagna della Maiella, Italy. *Sedimentary Geology*, 123(1-2): 103-127.

Vescogni A., Bosellini F.R., Papazzoni C.A., Giusberti L., Roghi G., Fornaciari E., Dominici S. & Zorzin R. (2016) - Coralgal buildups associated with the Bolca Fossil-Lagerstätten: new evidence from the Ypresian of Monte Postale (NE Italy). *Facies*, 62: 1-20.

Vicedo V. & Robles-Salcedo R. (2022) - Late Cretaceous larger rotaliid foraminifera from the westernmost Tethys. *Cretaceous Research*, 133: 105137.

Vitale S. & Ciarcia S. (2022) - The dismembering of the Adria platforms following the Late Cretaceous-Eocene abortive rift: a review of the tectono-stratigraphic record in the southern Apennines. *International Geology Review*, 64(20): 2866-2889.

Vršič A., Gawlick H.J., Schlagintweit F., Machaniec E. & Gharsalla M. (2021) - Age, microfacies and depositional environment of the Middle to Late Paleocene shallow-marine carbonates in the Sirt Basin of Libya (Upper Sabil Formation): "Are Intisar domal structures pinnacle reefs?". *Facies*, 67(4): 27.

Wade B.S., Pearson P.N., Berggren, W.A. & Pälike H. (2011) - Review and revision of Cenozoic tropical planktonic foraminiferal biostratigraphy and calibration to the geomagnetic polarity and astronomical time scale. *Earth-Science Reviews*, 104(1-3): 111-142.

Wilkinson C. (2004) - Status of Coral Reefs of the World: 2004. Global Coral Reef Monitoring Network and Australian Institute of Marine Science, Townsville, Australia, 557 pp.

Wood R. (1995) - The changing biology of reef-building. *Palaios*, 10: 517-529.

Zachos J., Pagani M., Sloan L., Thomas E. & Billups K. (2001) - Trends, rhythms, and aberrations in global climate 65 Ma to present. *Science*, 292(5517): 686-693.

Zamagni J., Mutti M. & Košir A. (2008) - Evolution of shallow benthic communities during the Late Paleocene–earliest Eocene transition in the Northern Tethys (SW Slovenia). *Facies*, 5: 25-43.

Zamagni J., Košir A. & Mutti M. (2009) - The first microbialite-coral mounds in the Cenozoic (Uppermost Paleocene) from the Northern Tethys (Slovenia): environmentally-triggered phase shifts preceding the PETM?. *Palaeogeography, Palaeoclimatology, Palaeoecology*, 274(1-2): 1-17.

Zamagni J., Mutti M. & Košir A. (2012) - The evolution of mid Paleocene-early Eocene coral communities: How to survive during rapid global warming. *Palaeogeography, Palaeoclimatology, Palaeoecology*, 317: 48-65.